

BETONGKONSTRUKSJONERS LIVSLØP

Et utviklingsprosjekt i samarbeid mellom offentlige byggherrer, industri og forskningsinstitutter



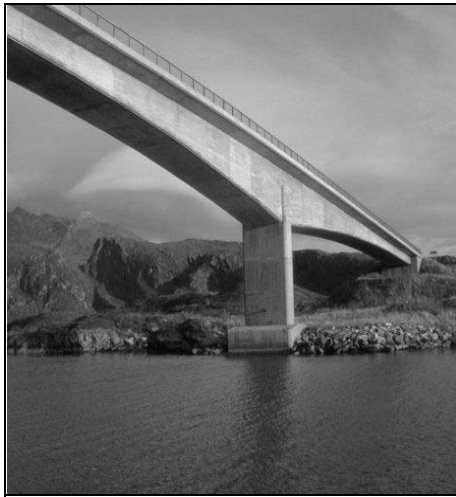
Deltakere:

Statens vegvesen (prosjektledelse), Forsvarsbygg, NORCEM A.S, Selmer Skanska AS, Sika Norge AS, Norges byggforskningsinstitutt, NTNU, SINTEF, NORUT Teknologi as

Rapport nr. 15

Nonlinear Finite Element Analysis of Deteriorated and Repaired RC Beams Aktivitet DP2 B3

Prosjektet er støttet av BA-programmet i Norges forskningsråd



BETONGKONSTRUKSJONERS LIVSLØP

Rapport nr. 15

**Nonlinear Finite Element Analysis of
Deteriorated and Repaired RC Beams.**

Aktivitet DP2 B3

Utgiver:
Statens vegvesen, Vegdirektoratet
Postadresse: Teknologivdelingen
Postboks 8142 Dep
0033 OSLO
Telefon: 02030
Telefaks: 22 07 38 66

FORFATTER(E):

Sand, B., NORUT Teknologi as

INTERN RAPPORT NR.

GRADERING

Åpen

ANTALL SIDER OG BILAG

15+34

RAPPORTNR./ ISBN.:

82-91228-20-5

DATO

Desember 2007

PROSJEKTLEDERE:

Finn Fluge og Bernt Jakobsen

KORT SAMMENDRAG

Armeringskorrosjon er den vanligste årsaken til nedbrytning av armerte betongkonstruksjoner. Korrosjon reduserer armeringstverrsnittet og påvirker heften mellom armering og betong. Dette kan redusere konstruksjonens stivhet og bæreevne. Reparasjon av skadde betongkonstruksjoner medfører at kloridinfisert betong fjernes før ny masse legges på. Dette kan redusere konstruksjonenes stivhet og bæreevne. Det kan derfor være usikkerhet knyttet til i hvilken grad reparasjoner basert på vanlige metoder fullt ut kan gjenskape konstruksjonens opprinnelige bæreevne. Det er således behov for pålitelige metoder for beregning av reststyrken til en reparert konstruksjon. I foreliggende rapport er ikke-lineære elementmetoder benyttet til å beregne bruddlast for skadde og reparerte betongbjelker.

Det er gjennomført numeriske analyser av både skadde og reparerte betongbjelker. Basert på Norsk Standard NS 3473 har betongbjelkene en beregnet lastkapasitet på 41,3 kN/m i bruddgrensetilstanden. Denne referanseverdien benyttes som sammenligningsgrunnlag for et sett bruddberegninger utført med elementmetoden.

For bjelker med 10% redusert armeringsareal og korrosjon jevnt virkende over et eksponert område på 50-70% av bjelkelengden ble beregnet bruddlast 1% til 3 % høyere enn lastkapasiteten etter NS 3473. For bjelker med 25% tverrsnittsreduksjon var beregnet bruddlast 86 til 89% av lastkapasiteten etter NS 3473.

Den numeriske simuleringen ga en kapasitet av uskadet bjelke som var 13% høyere enn kapasiteten beregnet etter NS 3473. Med en reduksjon av armeringstverrsnittet med 10% ble kapasiteten lik 89-90% av kapasiteten for intakt bjelke. Tilsvarende restkapasiteter for 25% tverrsnittsreduksjon var 75-78% av intaktkapasiteten. Dette viser at for de undersøkte bjelkene var kapasiteten redusert svært nær proporsjonalt med korrodert tverrsnitt.

Videre er det gjennomført simulering av bjelker utsatt for både pitting og samtidig jevnt virkende korrosjon. Armeringstverrsnittet ble over 50% av bjelkelengden redusert med 25% og med 38% i pittingsonen. Beregnet bruddlast for dette tilfellet utgjør 77% av lastkapasiteten etter NS 3473. Dette tilsvarer 68% av kapasiteten til uskadet bjelke, hvilket samsvarer godt med 38% tverrsnittsreduksjon forårsaket av pitting.

STIKKORD	NORSK	ENGLISH
	Betong	Concrete
	Korrosjon	Corrosion
	Elementanalyse	Finite Element Analysis
	Heftfasthet	Bond strength

Rapport	Nr. 15	Nonlinear Finite Element Analysis of Deteriorated and Repaired RC Beams.
Prosjekt		Betongkonstruksjoners livsløp Et utviklingsprosjekt i samarbeid mellom offentlige byggherrer, industri og forskningsinstitutter.
Aktivitet	DP2 B3	Vedlikeholds- og oppgraderingsmetoder Oppgraderingsmetoder Styrkeberegning av skadde og reparerte konstruksjoner
Deltagere		Statens vegvesen (prosjektledelse), Forsvarsbygg, NORCEM A.S, Selmer-Skanska AS Sika Norge AS Norges byggforskningsinstitutt, NTNU, SINTEF, NORUT Teknologi as Prosjektet er støttet av BA-programmet i Norges forskningsråd ISSN 1502-2331 ISBN 82-91228-20-5 50 eksemplarer trykt av Statens vegvesen, Teknologidivisjonen © Statens vegvesen 2007
Adresse		Vegdirektoratet, Teknologidivisjonen Postboks 8142 Dep N-0033 Oslo, Norway
Telefon		+ 47 02030
Telefax		+ 47 22 07 38 66
Emneord		Betong Korrosjon Elementanalyse Heftfasthet
Key words		Concrete Corrosion Finite Element Analysis Bond strength

FORORD

Fokus er i løpet av de senere årene flyttet fra bygging av nye konstruksjoner over mot forvaltning hvor det legges større vekt på problemstillinger knyttet til drift, vedlikehold og gjenbruk av eksisterende konstruksjoner.

Prosjektet "Betongkonstruksjoners livsløp" er knyttet opp mot denne typen utfordringer som en samlet bygg- og anleggsbransje står overfor. Kravene til bygg- og anleggskonstruksjoner er at de skal være funksjonelle og kostnadseffektive. Offentlige byggherrer forvalter og vedlikeholder et stort antall konstruksjoner som skal møte samfunnets krav til:

- sikkerhet
- kvalitet/økonomi
- miljø

Det ble de siste årene av 90-tallet lagt ned et betydelig arbeid i prosjektet "Bestandige betongkonstruksjoner". Av resultatene fra dette prosjektet og erfaringene fra prosjektet "OFU Gimsøystraumen" fremgår det klart at beslutningen om å bygge bestandige betongkonstruksjoner må tas tidlig i planleggingsfasen og at det er behov for enkelt å kunne verifisere prosjekteringsforutsetningene.

"Betongkonstruksjoners livsløp" bygger videre på forannevnte prosjekter. Hovedvekten er lagt på klart formulerte forskningsoppgaver som dels konkretiserer eksisterende kunnskap og dels fyller hull i kunnskapsgrunnlaget. Aktivitetene er valgt innenfor en ramme som omfatter alle faser fra planlegging til riving og gjenbruk.

Prosjektets hovedmålsetning har vært:

Kostnadseffektive og miljøgunstige betongkonstruksjoner

med følgende delmål:

- Identifisere hovedparametre i levetidsmodellene og kalibrere dem mot feltefaringer
- System for vurdering av vedlikeholdstiltaks levetid
- System for instrumentell overvåking av betongkonstruksjoners tilstandsutvikling
- Kunnskapsformidling gjennom normarbeid, kurs og internasjonale nettverk

Prosjektets sluttprodukter er:

- Grunnlag for veiledninger og regler for levetidsprosjektering
- Akseptkriterier for bedømmelse av betongkonstruksjoners bestandighet
- Datagrunnlag til bruk i standardiseringsarbeid og som inngangsdata til europeisk nettverksarbeid
- Kunnskap og kompetanse knyttet til sensorteknologi, måleteknikk, "intelligent" instrumentell overvåking, katodisk beskyttelse etc., hvor industripartnerne gis mulighet til å utnytte resultatene kommersielt

Prosjektet har bestått av flere større og mindre aktiviteter gruppert i følgende delprosjekter:

- DP1. Levetidsprosjektering
 - A. Datainnsamling
 - B. Levetidsmodeller
- DP2. Vedlikeholds- og oppgraderingsmetoder
 - A. Vedlikeholdsmetoder
 - B. Oppgraderingsmetoder
 - C. Rustfri armering
- DP3. Måleteknikk

Aktivitetene i prosjektet er basert på enkeltforslag fra prosjektdeltakerne. Hvor aktivitetene hadde fellestrekk, kunne levere resultater til, eller benytte resultater fra andre aktiviteter ble dette identifisert ved oppstarten av prosjektet og nødvendig koordinering foretatt. Ellers er aktivitetene styrt meget selvstendig.

Prosjektet startet høsten 1999 og ble avsluttet høsten 2001. Prosjektet har vært støttet av BA-programmet i Norges forskningsråd med NOK 1 mill i hvert av årene 1999 og 2000.

I tillegg til støtten fra Norges forskningsråd har det vært ytet en betydelig egeninnsats fra deltakerne i form av personalinnsats og kjøp av FoU-tjenester. Prosjektkostnadene per 31-12-00 var NOK 7,25 mill, hvorav NOK 2,7 mill var benyttet til kjøp av FoU-tjenester fra forskningsinstitutter og NOK 0,5 mill fra konsulent. I år 2001 ble det kjøpt tjenester for NOK 1,7 mill som i sin helhet ble finansiert av prosjektdeltagerne. Samlede prosjektkostnader ved avslutningen av prosjektet er ca. NOK 9 mill.

Prosjektet har hatt følgende deltakere:

Statens vegvesen
Forsvarsbygg
NORCEM A.S
Selmer Skanska AS
NTNU
SINTEF
Sika Norge AS
Norges byggforskningsinstitutt
NORUT Teknologi as

I tillegg har prosjektet samarbeidet med Det Norske Veritas og ARMINOX, som alle har bidratt med egeninnsats.

Det er knyttet to dr. gradsstudenter til prosjektet.

Prosjektet mottok i juni 2000 et 3 års dr.grad stipendium. Stipendiat ble tilsatt 01-01-2001.

Prosjektet har vært ledet av Vegdirektoratet. Prosjektledelsen, som har bestått av Finn Fluge Vegteknisk avdeling, Vegdirektoratet og Bernt Jakobsen, Aadnesen a.s, har rapportert til en styringskomite som har bestått av representanter fra prosjektdeltakerne. Styringskomiteen har vært samlet to ganger årlig eller ved behov og har fastlagt mål og hovedstrategier.

SUMMARY

Corrosion of reinforcement is the most common cause for deterioration of concrete structures. Many concrete structures, exposed to thawing salt and salt spray, show serious damages which have brought maintenance and repair into focus.

Despite that new repair methods as cathodic protection etc. are available, the main part of repair works is still performed by chiselling and removal of chloride contaminated concrete. Corrosion causes reduced cross-section of the steel reinforcement and reduced bond strength between steel and concrete which in turn have significant effects on the stiffness and ultimate strength of the structure. Additionally, the load bearing capacity of the structure may not be fully restored when normal repair methods are used. Hence, there is a need for accurate and reliable methods for determining the residual strength of deteriorated and repaired concrete structures.

The present report deals with computation of the load bearing capacity of concrete beams by means of non-linear finite element simulations. The numerical simulations have been performed on both deteriorated and repaired, simply supported beams. The beams were 8 meter long and had a cross section $b \times h = 250 \times 600$ mm. The tension reinforcement was four bonded bars of diameter 25 mm, while three bars of diameter 10 mm acted in compression and the stirrups were diameter 10 mm at 500 mm distance.

The following input data was used in the computations, reinforcement of type B500NC and concrete of grade C35. Design of beams based on NS 3473 gives a load capacity in the ultimate limit state (ULS) of 41,3 kN/m, and is used as reference to compare results obtained from the finite element analyses.

Finite element simulations on basis of 10% and 25% reduction of the reinforcement cross section and uniform corrosion acting over an exposed beam length of 50% to 70% demonstrate that the computed ultimate load decreases with increased corrosion depths and to some extent also with increased beam lengths.

For beams with 10% reduction in the cross section of the tensile reinforcement and exposed beam length below 60% the computed ultimate loads are 1% to 3% higher than the load capacity based on NS 3473. When increasing the exposed part of the beam length to 67% the obtained computed ultimate load decreases to 97% compared to the NS 3473 value. For the last case the failure mode was debonding failure while the other beams failed in compression.

Beams with 25% reduction of the steel area had correspondingly a computed ultimate load of 86% to 89% compared with NS 3473, where this variation was due to different lengths of the exposed area.

The numerical simulation gave a capacity of the intact beam that was 13% higher than its ultimate capacity according to NS 3473. With a reduction of the cross-section of the tension bars of 10% the ultimate capacity of the beam was reduced to 89-90% of the intact capacity. The corresponding rest capacity for 25% reduction was 75-78% of the intact capacity. This shows that for the beams investigated the capacity was reduced approximately in proportion to the reduction in the cross-section of the tension steel.

The deflections of the beams were decreasing when the exposed beam length was increasing.

Splicing of the tensile reinforcement had only minor effects on the computed ultimate load, but some differences in the distribution of the shear stress slip along the beams were observed.

Finite element simulations of deteriorated and repaired beams attacked by pitting and uniform corrosion were also performed. The tensile bar cross-section, due to uniform corrosion was reduced with 25% acting over a beam length of 50% and with 38% due to pitting in the mid section of the beams. Obtained computed ultimate load was 77% compared to NS 3473. This is 68% of the capacity of the intact beam and corresponds fairly well with the 38% reduction of the reinforcement cross-section in the pitting zone. Deflections were considerably reduced.

- Rapport nr. 5:** TITTEL: Statistisk beregning av levetid for betongkonstruksjoner utsatt for kloridinntrengning.
Aktivitet: DP1 B1
Utgiver: Statens vegvesen, Vegdirektoratet, Vegteknisk avdeling. SINTEF. Rapport nr. STF22 A01613.
Forfattere: Hynne, T., Leira, B.J., Carlsen, J.E. og Lahus, O.
ISSN 1502-2331
ISBN 82-91228-10-8
Sider: 14+59+3 vedlegg
Dato: Februar 2003
- Rapport nr. 6:** TITTEL: Dimensjoneringsformat for kloridbestandighet.
Aktivitet: DP1 B1
Utgiver: Statens vegvesen, Vegdirektoratet, Vegteknisk avdeling. SINTEF. Rapport STF22 A02601.
Forfattere: Leira, B.J.
ISSN 1502-2331
ISBN 82-91228-11-6
Sider: 14+36+ 1 vedlegg
Dato: Februar 2003
- Rapport nr. 7:** TITTEL: Pålitelighetsmetodikk ved bruk av FDV og levetidsberegninger.
Aktivitet: DP1 B2
Utgiver: Statens vegvesen, Vegdirektoratet, Vegteknisk avdeling. Aas-Jakobsen. Rapp 6943-01.
Forfattere: Larsen, R.M.
ISSN 1502-2331
ISBN 82-91228-12-4
Sider: 14 + 67
Dato: Februar 2003
- Rapport nr. 8:** TITTEL: Effekt av reparasjon på levetid: Eksempelstudie fra Gimsøystraumen.
Aktivitet: DP1 B3
Utgiver: Statens vegvesen, Vegdirektoratet, Vegteknisk avdeling. SINTEF. Rapport nr. STF22 A01607.
Forfattere: Hynne, T. og Leira, B.J.
ISSN 1502-2331
ISBN 82-91228-13-2
Sider: 12 + 22 + 7 vedlegg
Dato: Oktober 2006

- Rapport nr. 9:** TITTEL: Bestandighet og levetid av reparerte betongkonstruksjoner.
Aktivitet: DP2 A2
Utgiver: Statens vegvesen, Vegdirektoratet, Vegteknisk avdeling. NORUT Teknologi as rapport NTAS F2001-36.
Forfattere: Arntsen, B.
ISSN: 1502-2331
ISBN: 82-91228-14-0
Sider: 14 + 20
Dato: Oktober 2006
- Rapport nr. 10:** TITTEL: Restlevetid – Kai Sjursøya.
Aktivitet: DP2 A3
Utgiver: Statens vegvesen, Vegdirektoratet, Vegteknisk avdeling. Selmer Skanska AS, rapport nr. B 01-01.
Forfattere: Carlsen, J.E.
ISSN: 1502-2331
ISBN: 82-91228-15-9
Sider: 12 + 15 + 7 vedlegg
Dato: November 2006
- Rapport nr. 11:** TITTEL: Feltforsøk Sykkylven bru.
Aktivitet: DP2 A4
Utgiver: Statens vegvesen, Vegdirektoratet, Vegteknisk avdeling. Selmer Skanska AS, rapport nr. B 01-02
Forfattere: Carlsen, J.E.
ISSN: 1502-2331
ISBN: 82-91228-16-7
Sider: 12 + 9 +30
Dato: Desember 2006
- Rapport nr. 12:** TITTEL: Strengthening Prestressed Concrete Beams with Carbon Fiber Polymer Plates.
Aktivitet: DP2 B1
Utgiver: Statens vegvesen, Vegdirektoratet, Vegteknisk avdeling. NTNU, Institutt for konstruksjonsteknikk.
Forfattere: Takacs, P.F. og Kanstad, T.
ISSN: 1502-2331
ISBN: 82-91228-17-5
Sider: 14 + 46 + 12
Dato: Desember 2006

- Rapport nr. 13:** TITTEL: Forsterking av betongsøyler med karbonfiberrev.
Aktivitet: DP2 B2
Utgiver: Statens vegvesen, Vegdirektoratet, Vegteknisk avdeling.
SINTEF. Rapport nr. STF22 A00718.
Forfattere: Thorenfeldt, E.
ISSN 1502-2331
ISBN 82-91228-18-3
Sider: 14 + 22 + 3 vedlegg
Dato: Desember 2006
- Rapport nr. 14:** TITTEL: Forankringskapasitet av CFAP-bånd limt til betong.
Aktivitet: DP2 B2
Utgiver: Statens vegvesen, Vegdirektoratet, Vegteknisk avdeling.
SINTEF. Rapport nr. STF22 A01618.
Forfattere: Thorenfeldt, E.
ISSN 1502-2331
ISBN 82-91228-19-1
Sider: 14 + 20 + 2 vedlegg
Dato: November 2007
- Rapport nr. 15:** TITTEL: Nonlinear Finite Element Analysis of Deteriorated and Repaired RC Beams
Aktivitet: DP2 B3
Utgiver: Statens vegvesen, Vegdirektoratet, Vegteknisk avdeling.
NORUT Teknologi as rapport NTAS F2001-31.
Forfattere: Sand, B.
ISSN 1502-2331
ISBN 82-91228-20-5
Sider: 15 + 34
Dato: Desember 2007
- Rapport nr. 16:** TITTEL: Styrkeberegning ved korrosjonsskader.
Aktivitet: DP2 B3
Utgiver: Statens vegvesen, Vegdirektoratet, Vegteknisk avdeling.
SINTEF. Rapport nr. STF22 A01619.
Forfattere: Stemland, H.
ISSN 1502-2331
ISBN 82-91228-21-3
Sider:
Dato:

- Rapport nr. 17:** TITTEL: Korrosjonsegenskaper for rustfri armering.
Aktivitet: DP2 C1
Utgiver: Statens vegvesen, Vegdirektoratet, Vegteknisk avdeling.
NTNU, Institutt for konstruksjonsteknikk.
Rapport R-9-01.
Forfattere: Vennesland, Ø.
ISSN 1502-2331
ISBN 82-91228-22-1
Sider:
Dato:
- Rapport nr. 18:** TITTEL: Heftforhold for rustfritt armeringsstål.
Aktivitet: DP2 C2
Utgiver: Statens vegvesen, Vegdirektoratet, Vegteknisk avdeling.
NTNU rapport.
Forfattere: Hofsøy, A., Sørensen, S.I. og Markeset, G.
ISSN 1502-2331
ISBN 82-91228-24-8
Sider:
Dato:
- Rapport nr. 19:** TITTEL: Service Life Design of Concrete Structures
Aktivitet: DP1 B4
Utgiver: Statens vegvesen, Vegdirektoratet, Vegteknisk avdeling.
Forfattere: Helland, S., Maage, M., Smepllass, S., Fluge, F.
ISSN 1502-2331
ISBN 82-91228-25-6
Sider:
Dato:
- Rapport nr. 20:** TITTEL: SLUTTRAPPORT
Aktivitet: -
Utgiver: Statens vegvesen, Vegdirektoratet, Vegteknisk avdeling.
Forfattere: Fluge, F. og Jakobsen, B.
ISSN 1502-2331
ISBN 82-91228-26-4
Sider:
Dato:

INNHOLDSFORTEGNELSE**FORORD**

iii

SUMMARY

v

RAPPORTOVERSIKT

vii

INNHOLDSFORTEGNELSE

xii

1. SAMMENDRAG

xiii

2. RAPPORT – innhold utgjøres av følgende vedlegg

NORUT Teknologi as rapport NTAS F2001-31, 2001
Sand, B.

”Nonlinear Finite Element Analysis of Deteriorated and Repaired RC Beams”.

SAMMENDRAG

Armeringskorrosjon er den vanligste årsaken til svekkelse og nedbrytning av armerte betongkonstruksjoner. Mange konstruksjoner eksponert for klorider, enten fra salting eller sjørokk, har fått til dels store skader. Som følge av dette har det de seneste årene vært fokusert på vedlikehold og reparasjon av slike konstruksjoner.

Selv om nye og moderne reparasjonsmetoder, basert på katodisk beskyttelse, re-alkalisering etc., er tatt i bruk, blir størsteparten av reparasjonene fortsatt utført ved å fjerne betong med kloridinnhold over en viss grense før ny masse legges på. Skal en slik metode være vellykket må all kloridholdig betong fjernes. Dette kan bety at betydelige mengder betong må fjernes. Videre vil korrosjon redusere armeringstverrsnittet og påvirke heftegenskapene mellom armering og betong. I sin tur vil dette redusere konstruksjonens stivhet og bæreevne.

Det er mye litteratur tilgjengelig knyttet til nedbrytningsmekanismer, reparasjonsmetoder og materialer, men lite som omhandler de styrkemessige sider av reparerte betongkonstruksjoner.

Reduksjonen av heften mellom armering og betong påvirker egenskapene til den reparerte betongkonstruksjonen og kan redusere bæreevnen når konstruksjonen igjen utsettes for full last. Det hefter usikkerhet ved i hvilken grad man ved reparasjoner utført etter vanlige metoder kan gjenskape konstruksjonens opprinnelige bæreevne.

Betongkonstruksjoner er ofte så komplekse at en realistisk beskrivelse av stivhets- og styrkeegenskapene når den kloridholdige betongen er fjernet krever omfattende datasimuleringer. Denne rapporten griper fatt i denne problematikken gjennom å beskrive hvordan ikke-lineære elementanalyser kan benyttes til å beregne bruddlaster for skadde og reparerte betongbjelker.

Bjelkenes lasthistorie beskrives og simuleres med ett i utgangspunktet ubeskadiget konstruksjonselement påkjent av full nyttelast. Etter korrosjon og heftnedbrytning samt fjerning av nyttelast og kloridinfisert betong utbedres bjelkene med reparasjonsmørtel før nye laster påføres.

I foreliggende arbeid er betongmaterialet modellert som et isotropt materiale med arbeidsdiagram på trykksiden i henhold til NS 3473. Det er valgt von Mises bruddkriterium. Oppførselen etter brudd er basert på plastisitetsteorien. På strekksiden er betongen lineær til strekkspenningen når strekkfastheten, da det dannes riss, og betongen kan deretter ikke overføre strekk normalt på risset. Armeringsstålet er beskrevet ved en standard elasto-plastisk modell.

Armeringskorrosjon, uttrykt som reduksjon av ståltverrsnittet kan, basert på måling av korrosjonshastighet, beregnes for ulike tidspunkt etter at korrosjon er initiert. Modellen gjør bruk av polarisasjonsteknikk og Farrady's lov og kan anvendes for både pitting og jevnt virkende korrosjon.

I analysen er det benyttet en empirisk formel for heftfastheten hvor det tas hensyn til korrosjonens nedbrytende virkning på heftegenskapene. Videre er det introdusert ikke-lineære fjærer i knutepunktene mellom elementene som beskriver armeringsstenger og betong. Man kan derved modellere sammenhengen mellom opptredende heftspenning og tilhørende glidning mellom armering og betong.

Effekten av redusert armeringstverrsnitt forårsaket av korrosjon er det tatt hensyn til ved å benytte to sett armeringselementer som hver for seg er koblet til betongelementene med ikke-lineære fjærer. Før korrosjonen initieres er begge armeringselementene fullt virksomme. Etter hvert som korrosjonen utvikler seg fjernes det ene settet og analysen fortsetter med redusert armeringstverrsnitt og reduserte heftegenskaper.

Det er gjennomført numeriske analyser av både skadde og reparerte fritt opplagte bjelker. Bjelkene hadde spennvidde 8,0 meter og tverrsnitt $b \times h = 250 \times 600$ mm. Strekkarmeringen som besto av 4 kamstål med diameter 25 mm var dels kontinuerlig gjennomgående og dels skjøtt med omfaringsskjøt i spennet. Trykkarmeringen var 3 kamstål med diameter 10 mm og bøyene var kamstål med diameter 10 mm i avstand 500 mm.

I beregningene er benyttet armering B500NC med dimensjonerende strekkfasthet 400 MPa og betong i fasthetsklasse C35 med dimensjonerende trykk og strekkfasthet på henholdsvis 16,0 MPa og 1,21 MPa. Bjelkens lastkapasitet i bruddgrensetilstanden var 41,3 kN/m, dimensjonert etter reglene i NS 3473. Denne verdien benyttes i det etterfølgende for å sammenlikne beregnede bruddlaster med lastkapasiteten i bruddgrensetilstanden.

Det er gjennomført analyser med 10% og 25% reduksjon av armeringstverrsnittet forårsaket av jevnt virkende korrosjon over et eksponert område som utgjør fra 50% til 70% av bjelkelengden. De numeriske simuleringene viser at beregnet bruddlast blir lavere når armeringstverrsnittet reduseres på grunn av korrosjon og bruddlasten reduseres også noe når lengden av klorideksponert strekkarmering øker.

For bjelker med 10% redusert armeringstverrsnitt i strekksonen og eksponert bjelkelengde som ikke overskrider 60% ble funnet bruddlast 1% til 3% høyere enn lastkapasiteten dimensjonert etter NS 3473. Ved å øke den klorideksponerte delen av bjelkelengden til 67% ble beregnet bruddlast redusert til 97% sammenlignet med lastkapasiteten etter NS 3473. Bruddformen gikk for det siste tilfellet over fra trykkbrudd til heftbrudd.

Bjelker med 25% reduksjon av armeringstverrsnittet hadde tilsvarende en beregnet bruddlast på 86% til 89% av lastkapasiteten basert på NS 3473 hvor denne variasjonen skyldes ulik lengde av klorideksponert armering.

Den numeriske simuleringen ga en kapasitet av uskadet bjelke som var 13% høyere enn kapasiteten beregnet etter NS 3473. Med en reduksjon av armeringstverrsnittet med 10% ble kapasiteten lik 89-90% av kapasiteten for intakt bjelke. Tilsvarende restkapasiteter for 25% tverrsnittsreduksjon var 75-78% av intaktkapasiteten. Dette viser at for de undersøkte bjelkene var kapasiteten redusert svært nær proporsjonalt med korrodert tverrsnitt. Når de klorideksponerte bjelkelengdene økte medførte dette økt nedbøyning.

Skjøting av strekkarmeringen med omfarings skjøt i spennet hadde liten effekt på bruddlasten, men det ble konstatert forskjeller knyttet til heftglidningen langs bjelken.

Videre er det gjennomført simulering av reparerte bjelker utsatt for både pitting og samtidig jevnt virkende korrosjon. Korrosjonsangrepet fra pitting ble konsentrert til ett område midt i bjelkespennet. Armeringstverrsnittet ble over 50% av bjelkelengden redusert med 25% og med 38% i pittingsonen.

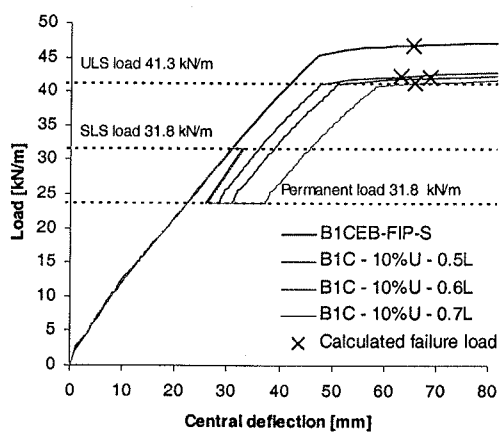
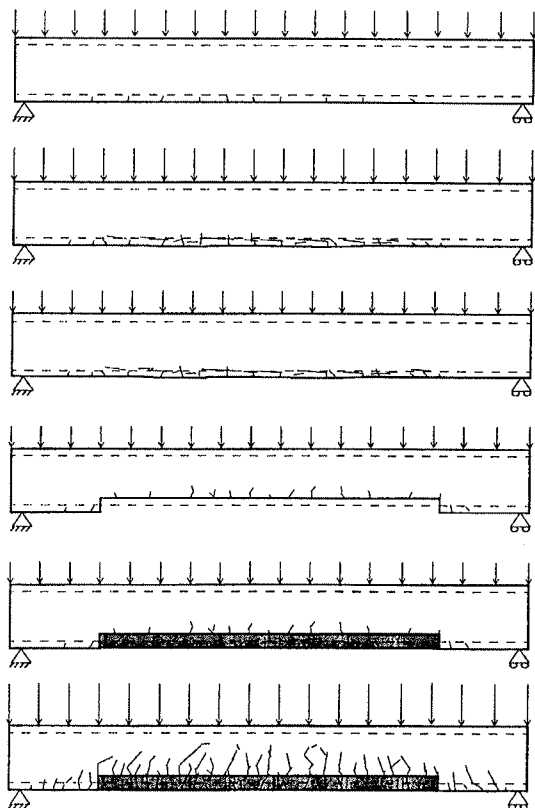
Beregnet bruddlast ble i dette tilfellet 31,8 kN/m, en verdi som tilsvarer størrelsen på lasten i bruksgrensetilstanden og utgjør 77% av lastkapasiteten etter NS 3473. Dette tilsvarer 68% av lastkapasiteten til uskadet bjelke, hvilket samsvarer godt med 38% tverrsnittsreduksjon i pittingsonen. Effekten av jevnt virkende korrosjon er ubetydelig når tverrsnittsreduksjonen er mindre enn reduksjonene som skyldes pitting i midtområdet. Nedbøyingene ved beregnet bruddlast var i dette tilfellet betydelig redusert.

NORUT Teknologi as

NONLINEAR FINITE ELEMENT ANALYSIS OF DETERIORATED AND REPAIRED RC BEAMS


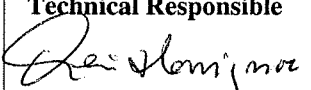
Author:

Bjørnar Sand



Narvik, septem ber 18th 2001

NORUT Teknologi as

Contracting institution: Vegdirektoratet, Vegteknisk avdeling	Contracting Ref. Finn Fluge
Author(s): Bjørnar Sand	Project No. 2066.03
	Document Type Report
	Document No. NTAS F2001-31
	ISSN ISBN
Document Title: NONLINEAR FINITE ELEMENT ANALYSIS OF DETERIORATED AND REPAIRED RC BEAMS	Status/Availability Open
	No. of Pages, Appendices 31
	Version 01 English
	Date 18.09.01
	Reviewed by 
	Technical Responsible 
Abstract/Summary <p>Corrosion of embedded steel reinforcement is the most common cause of deterioration of reinforced concrete structures. Repair of damaged concrete members usually implies removal of chloride contaminated concrete and , thereby exposing the tensile reinforcement bars in certain areas. Corrosion causes reduced cross section area of the steel bars and reduced bond strength, which may have significant effects on the stiffness and ultimate strength of the structure. The load-carrying capacity of may not be fully restored by commonly employed repair techniques. All of this exposes the need for accurate and reliable methods for determining the residual strength of deteriorated and repaired concrete structures. The present report focuses attention on the calculation of load-carrying capacity of deteriorated and repaired concrete beams by means of nonlinear finite element simulations.</p> <p>Numerical examples in the form of deteriorated and repaired concrete beams with or without spliced tensile reinforcement were presented. Using Norwegian codes, the beam was designed to sustain an ultimate limit load (ULS) of 41.3 kN/m. The cross section of the tensile reinforcement were reduced by 10% and 25% due to uniform corrosion and the tensile reinforcement were exposed over a length of 50% to 70% of the span of the beams. For beams with 10% reduction of the tensile reinforcement, the calculated ultimate load were 1% to 3% greater than the ULS load of 41.3 kN/m, while beams with 25% reduction only could sustain a load which were in the range between 86% to 89% of the ULS load. Finite element simulations of beams attacked by uniform corrosion and pitting were also carried out. The cross section area of the tensile reinforcement were reduced by 25%. In addition, the cross section of the tensile reinforcement were also reduced by 38% due to pitting. The pits were located at the centre of the beams. The calculated ultimate load was equal to the SLS load of 31.8 kN/m which is only 77% of the ULS load of 41.3 kN/m.</p>	
Keywords finite element analysis, concrete, corrosion, bond	
Notices	
Distribution	

Address:
 Lodve Langes gt 2
 P. O. Box 250
 N-8504 Narvik
 Norway

Telephone: +47-76 96 53 51
 Telefax: +47-76 96 53 51

e-mail: info@tek.norut.no
 internet: http://www.norut.no/teknologi

CONTENTS

1.	INTRODUCTION	1
2.	DETERIORATION AND REPAIR HISTORY	2
3.	CONSTITUTIVE MODELLING OF CONCRETE AND REINFORCEMENT .	3
4.	CORROSION OF REINFORCING BARS	4
4.1	Reduction of reinforcing bar section due to corrosion	4
4.2	Relation between corrosion and bond deterioration	6
4.3	Bond stress-slip models	6
4.4	Finite element modelling of debonding	9
5.	NUMERICAL EXAMPLES	10
5.1	Deteriorated and repaired beams attacked by uniform corrosion	10
5.2	Deteriorated and repaired beams attacked by uniform corrosion and pitting	20
5.3	Deteriorated and repaired beams with spliced reinforcement attacked by uniform corrosion	23
5.4	Deteriorated and repaired beams with spliced reinforcement attacked by uniform corrosion and pitting	27
6.	CONCLUDING REMARKS	29
7.	REFERENCES	31

1. INTRODUCTION

During recent years, widespread problems of deterioration of reinforced concrete infrastructure have been experienced in many countries. The principal cause of this deterioration is corrosion of embedded reinforcement resulting from the diffusion of chlorides through the concrete cover. Bridge structures are particularly affected due to the use of de-icing salts in the winter season. However, concrete structures in marine environment have also suffered from severe deterioration. In this latter case, chlorides are transported to the concrete surface by the combined action of wind and waves.

As a result of the deterioration of concrete structures, repair and maintenance efforts have increased rapidly in recent years. The annual costs of repair of concrete members are likely to continue to rise in the coming years. The problem of reinforcement corrosion and subsequent deterioration of concrete has no simple or unique solution, and significant research efforts are being spent in order to develop new, innovative methods for protection or reinstatement of concrete structures. Among the most widely used techniques are cathodic protection systems, and desalination or realcalization by means of electro-chemical procedures. Nevertheless, the majority of the repair work continues to be performed by removing the chloride contaminated concrete around the corroded reinforcement and replacing it by a suitable concrete or mortar. For this method to be successful, all contaminated concrete must be removed. In many cases, this may require the braking out of concrete over wide areas and thereby significantly reducing the load carrying capacity of the structure.

A large number of research reports and papers have been devoted to the non-structural aspects of deterioration of reinforced concrete. The causes and mechanisms of deterioration, equipment and procedures for inspection, durability testing methods, and selection of repair materials and repair procedures have been comprehensively dealt with in the literature. On the other hand, the structural consequences or effectiveness of repairs of concrete members have received little attention. This is somewhat surprising since the full integrity of the structure is implied after the repair work has been completed and the structure is again subjected to the design loads. In addition, removal of contaminated concrete and the associated debonding of steel reinforcement may significantly reduce the load-carrying capacity of the structure, which should be taken into account when selecting the sequence and amount of patch repairs.

Practical concrete structures are generally so complex that realistic predictions of their stiffness or strength after the chloride contaminated material has been removed, usually require the use of computerized discretization methods. The present report addresses this question by describing how nonlinear finite element analysis can be effectively utilized to obtain realistic predictions of failure loads of repaired RC beams.

2. DETERIORATION AND REPAIR HISTORY

The mechanical behavior of reinforced concrete structures is generally path-dependent. For a deteriorating concrete structure which is subjected to partial unloading during repair and subsequently reloaded, the dependence on strain history is even more pronounced. Consequently, nonlinear finite element simulations must represent a close approximation of a realistic or true deterioration and repair sequence of a concrete structure. To this end, a special procedure was developed by Horrignoe and Tørlen [1, 2]. The main features of this approach can be explained from Figure 2.1, where a simply supported beam is used for illustration.

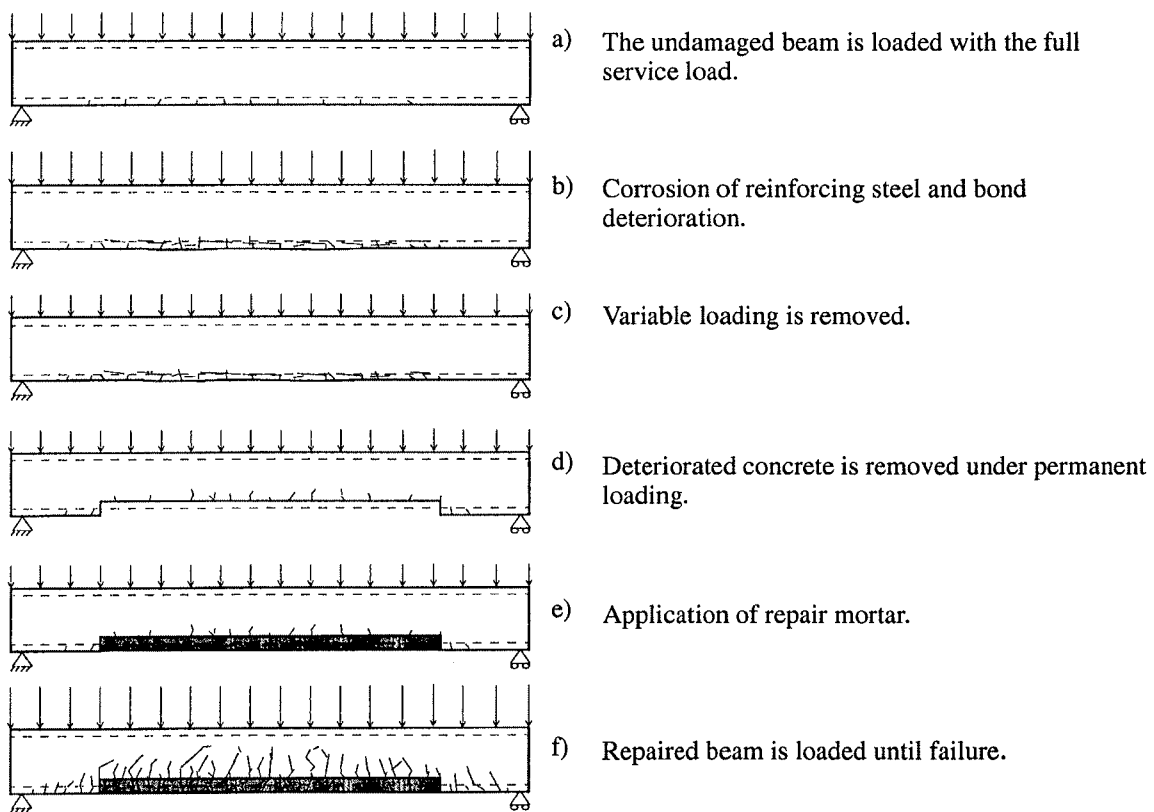


Figure 2.1 Tracing the deterioration and repair history of concrete beam.

First, the discretized model of the beam is incrementally loaded up to full service load, during which cracking occurs (Figure 2.1a). In this condition, corrosion of the reinforcing steel takes place over a given portion of the beam (Figure 2.1b). This is accomplished by gradually reducing the area of the affected steel bars and reducing the bond strength. This implies changing the stiffness of the structure while loaded, hence, an iterative procedure is required to reach a new equilibrium position. The structure is then taken out of service and the variable component of the loading is removed, so that only the permanent load remains (Figure 2.1c). Chloride contaminated concrete is removed, thereby exposing the tensile reinforcement over a portion $L_{\text{exp}} = \alpha \cdot L$ of the span L (Figure 2.1d). This is achieved by removing the associated

elements from the model. The contaminated concrete is replaced by a cement-based mortar by adding new elements, with different material properties, to the discretized model (Fig. 1 e). These two steps require equilibrium iterations. The mortar is strain-free, whereas the surrounding concrete has been subjected to loading and partial unloading resulting in permanent straining (i.e., cracking). Finally, the repaired beam is gradually loaded until failure occurs (Fig. 1f). The associated load-displacement diagram is illustrated in Figure 2.2. If it is decided to strengthen the beam either by adding extra reinforcing bars or by externally applied CFRP material, this can easily be included in the present method.

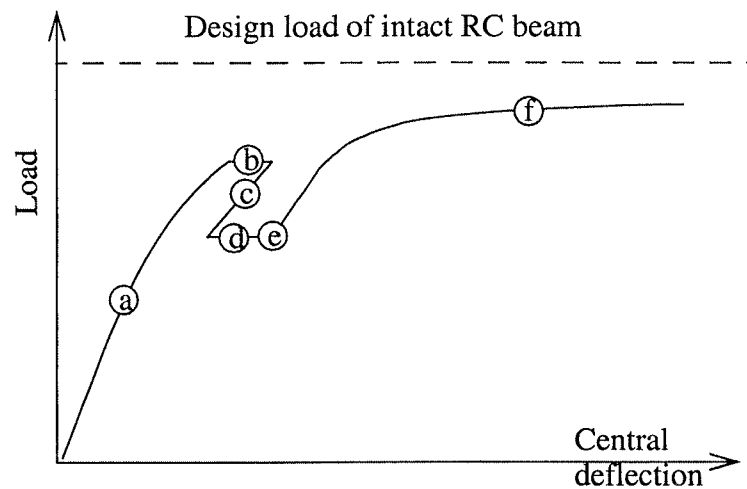


Figure 2.2 Load-deflection curve for beam loaded and repaired according to Figure 2.1.

3. CONSTITUTIVE MODELLING OF CONCRETE AND REINFORCEMENT

Assuming concrete to be isotropic, a number of failure criteria have been developed to represent compressive failure. In the present investigation the compressive strength of concrete is described with von Mises failure criterion and the post crushing behavior of concrete is described based on the theory of plasticity and the uniaxial compressive stress-strain approximation is shown in Figure 3.1. Using von Mises failure criterion is valid when the state of stress is mainly uniaxial as in the case of flexural bending of RC beams.

In tension, concrete can be approximated as a linear, brittle material. Cracking is defined to occur if the maximum principal stress exceeds the uniaxial tensile strength of concrete. After cracking has taken place, the material cannot sustain tensile, normal stresses perpendicular to the crack. This condition is introduced by modifying the stress-strain relation. The crack model allows shear stresses to be transmitted across the crack by defining the shear strength of cracked concrete to be a constant fraction of the shear strength in the uncracked state. In the general three-dimensional case, three independent crack planes may form at a material point.

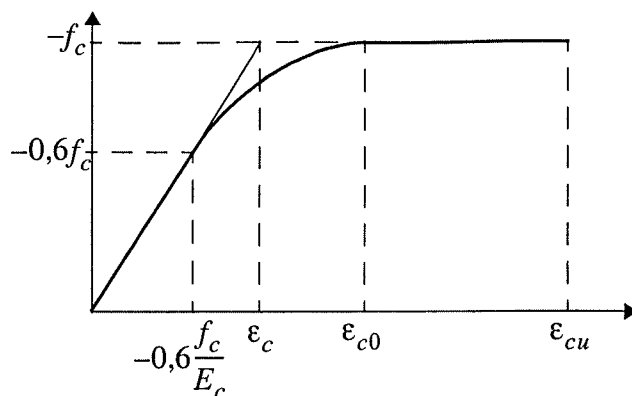


Figure 3.1 Uniaxial compressive stress - strain approximation with von Mises failure criterion as specified in NS 3473 [8].

The associated stress-strain relation depends on the orientation of cracks as well as whether cracks are open or closed. In the finite element formulation, cracking is restricted to the integration points of the individual elements, i.e., so-called smeared cracking.

Reinforcing bars are made of mild steel with a well-defined yield strength. Hence, a standard elasto-plastic model can be adopted for the steel reinforcement. The material behavior of the reinforcing steel is then described by the yield strength f_{sy} , the elasticity modulus E_s and the elasto-plastic tangent modulus E_s^T of steel.

4. CORROSION OF REINFORCING BARS

4.1 Reduction of reinforcing bar section due to corrosion

Corrosion in either carbonated or chloride contaminated concrete reduces the reinforcing bar section. Whereas uniform or homogenous attack penetration at the bars occurs in carbonated concrete, chlorides may produce localized attack often referred to as pitting and cause a significant section decrease. The bar attack penetration be estimated from the measurement of corrosion rate and using the polarization technique [3] and apply Farrady's law:

$$x = 0,0115 I_{corr} t \quad (4.1)$$

where x is the attack penetration in mm, t is the time in years elapsed since the aggressive reacted the reinforcement and I_{corr} is the average value of the corrosion rate in $\mu A/cm^2$ during time t . Usually the corrosion rate ranging between 0.1-0.2 and 1-2 $\mu A/cm^2$. The residual rebar diameter ϕ can be estimated from the nominal diameter ϕ_0 by:

$$\phi_R = \phi_0 - \alpha x \quad (4.2)$$

where α is a coefficient which depends on the type of attack. When uniform corrosion occurs, α is equal to 2, see Figure 4.1a. The residual rebar diameter due to uniform corrosion ϕ_R^u is then

$$\phi_R^u = \phi_0 - 2x \quad (4.3)$$

However, when localized corrosion occurs as shown in Figure 4.1b, α may reach values up to 4-8. A conservative value of the residual section at pits ϕ_R^p can then be predicted by:

$$\phi_R^p = \phi_0 - \alpha x \quad (4.4)$$

When the tensile reinforcement in a beam is attacked by uniform corrosion, the residual cross section area of tensile reinforcement A_{sR}^u can then be estimated from

$$A_{sR}^u = n \frac{\pi \phi_R^u}{4} \quad (4.5)$$

where n is the number of the tensile reinforcing bars in the concrete beam. If pitting occurs, the residual cross section area of the tensile reinforcement A_{sR}^{up} can be estimated by

$$A_{sR}^{up} = (n-1) \frac{\pi \phi_R^u}{4} + \frac{\pi \phi_R^p}{4} \quad (4.6)$$

Here it is assumed that only one rebar is attacked by pitting and the remaining rebars are attacked by uniform corrosion.

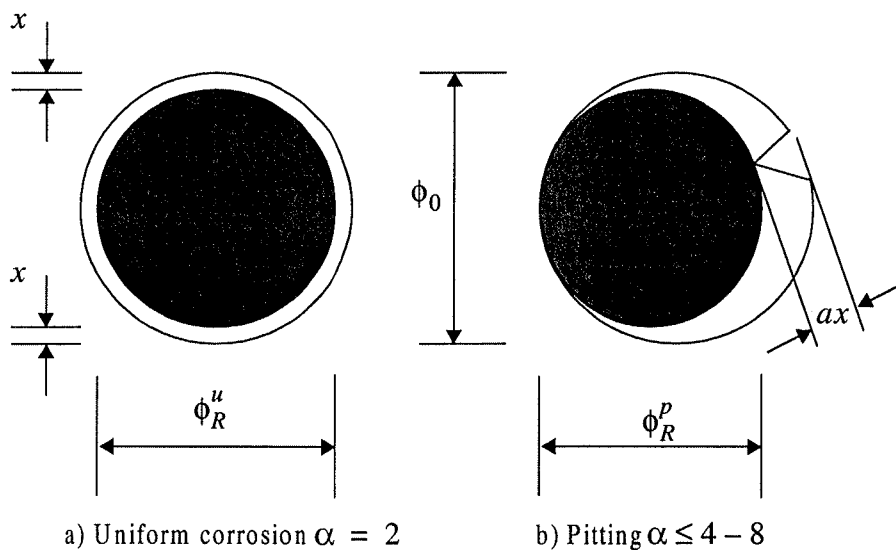


Figure 4.1 Residual reinforcing bar section. a) Uniform corrosion. b) Pitting.

4.2 Relation between corrosion and bond deterioration

To model the variation of bond strength τ_{max}^c with corrosion levels x , a relation has to be considered of the form:

$$\tau_{max}^c = \tau_{max}^c(x) \quad (4.7)$$

where τ_{max}^c is the bond strength and x is the corrosion level given by Eq. (4.1). Bond deterioration in the post-cracking regime may be estimated using the empirical formula by Rodriguez et al. [4], as it considers the presence of ties, the negative effects of corrosion of the selfsame ties, and the positive effect of support reaction confinement:

$$\tau_{max}^c = \tau_c + \tau_s = 0,6 \left(0,5 + \frac{C}{\phi_0} \right) f_{ct} (1 - \beta x^\mu) + k \frac{A_{s,s} f_{y,s}}{S_s \phi_s} \quad (4.8)$$

with

$$k \frac{A_{s,s} f_{y,s}}{S_s \phi_s} \leq 1,7 \text{ MPa} \quad (4.9)$$

The bond strength τ_{max}^c is a contribution from the concrete τ_c and stirrups τ_s . The contribution from the concrete is dependent of the cover to rebar ratio C/ϕ_0 , the tensile strength of the concrete f_{ct} and the attack penetration depth x . The contribution from the stirrups is dependent of the cross section of stirrups $A_{s,s}$, the yield strength of the stirrups $f_{y,s}$ and the distance between stirrups S_s . The constants β , μ and k involved in Eq. (4.8) have to be fitted with experimental results. The relation given by Eq. (4.8) has been obtained fitting bond test results to determine the constants β , μ and k , with varying concrete cover and amount of stirrup confinement [4]. This expression has been developed considering the results from pullout tests with concrete with compressive strength equal to 40 MPa, when applying a current density $I_{corr} = 0,1 \text{ mA/cm}^2$ to accelerate the corrosion of steel. The main bar diameter was $\phi_0 = 16 \text{ mm}$ and stirrup diameter $\phi_8 \text{ mm}$ with spacing S equal to 70 mm and the concrete cover was $C = 24 \text{ mm}$. The resulting values of the constants β , μ and k was 0.26, 0.1 and 0.163, respectively.

4.3 Bond stress-slip models

A local bond stress-slip model is proposed in CEB-FIP Model code 1990 [5] as shown in Figure 4.2a. The first curved part refers to the stage in which the ribs penetrate into the mortar matrix, characterized by local crushing and micro-cracking. After the bond strength τ_{max} is reached, the horizontal level occurs only for confined concrete, referring to advanced crushing and shearing off of the concrete between the ribs. The decreasing branch refers to the reduc-

tion of bond resistance due to occurrence of splitting cracks along bars. The horizontal part represents the residual bond capacity τ_f , which is maintaining by virtue of a minimum transverse reinforcement, keeping a certain degree of entirety intact.

The bond stress between concrete and reinforcing bars can be expressed as a function of the relative displacement S according to Eqs. (4.10) to (4.13):

$$\tau = \tau_{\max} \left(\frac{S}{S_1} \right)^\alpha \quad \text{for } 0 \leq S \leq S_1 \quad (4.10)$$

$$\tau = \tau_{\max} \quad \text{for } S_1 < S \leq S_2 \quad (4.11)$$

$$\tau = \tau_{\max} - (\tau_{\max} - \tau_f) \left(\frac{S - S_2}{S_3 - S_2} \right) \quad \text{for } S_2 < S \leq S_3 \quad (4.12)$$

$$\tau = \tau_f \quad \text{for } S_3 > S \quad (4.13)$$

The bond strength τ_{\max} for reinforcement without corrosion is function of the uniaxial compressive strength of the concrete f_c for ribbed bars the bond strength and residual bond strength is according to CEB-FIP given as

$$\tau_{\max} = 2\lambda \sqrt{f_c} \quad (4.14)$$

Here λ is a reduction factor which account for cracking of the concrete and can be estimated from the following expression:

$$\lambda = 0,2 \frac{x_w}{\phi_0} \leq 1 \quad (4.15)$$

Where x_w is the average distance between the cracks and ϕ_0 is the rebar diameter. The residual bond strength τ_f is set equal to 15% of the bond strength τ_{\max} , that is:

$$\tau_f = 0,15\tau_{\max} \quad (4.16)$$

For ribbed bars the parameter α can be set equal to 0.4 and the values of the parameters S_1 , S_2 and S_3 are given as

$$S_1 = \lambda 0,6 \text{ mm} \quad (4.17)$$

$$S_2 = \lambda 0,6 \text{ mm} \quad (4.18)$$

$$S_3 = \lambda 1,0 \text{ mm} \quad (4.19)$$

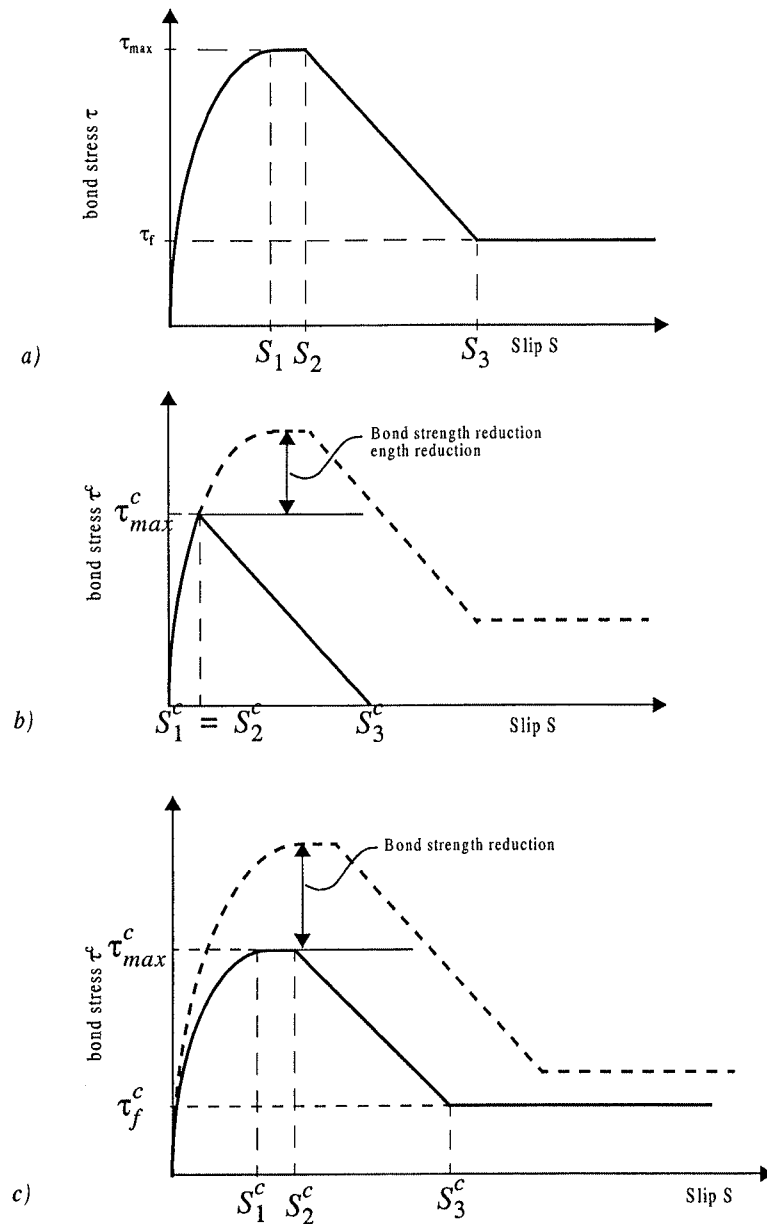


Figure 4.2 Bond stress-slip models. a) CEB-FIP model for reinforcement without corrosion, CEB-FIP [5]. b) Model proposed by Castellani [6] for reinforcement attacked by uniform corrosion. c) Model proposed by Tørnlen et al. [7] for reinforcement attacked by uniform corrosion.

Castellani et al. [6] modified the stress-slip model proposed in CEB-FIP Model code 1990 [5] to consider also corrosion effects. The bond stress-slip relation is shown in Figure 4.2b. The bond stress τ^c can be calculated from Eqs. (4.20) to (4.23):

$$\tau^c = \tau_{max}^c \left(\frac{S}{S_1^c} \right)^\alpha \quad \text{for } 0 \leq S \leq S_1^c \quad (4.20)$$

$$\tau^c = \tau_{max}^c \quad \text{for } S_1^c < S \leq S_2^c \quad (4.21)$$

$$\tau^c = \tau_{\max}^c - (\tau_{\max}^c - \tau_f^c) \left(\frac{S - S_2^c}{S_3^c - S_2^c} \right) \quad \text{for } S_2^c < S \leq S_3^c \quad (4.22)$$

$$\tau = \tau_f^c \quad \text{for } S \geq S_3^c \quad (4.23)$$

The bond strength τ_{\max}^c for reinforcement with corrosion is given by Eq. (4.8) and the residual bond strength τ_f^c is set equal to zero and the parameter α can be set equal to 0.4. It is assumed that the decreasing branches in Figure 4.2a and b are parallel. Then the parameters S_1^c , S_2^c and S_3^c are given as

$$S_1^c = \left(\frac{\tau_{\max}^c}{\tau_{\max}} \right)^{\frac{1}{\alpha}} S_1 \quad (4.24)$$

$$S_2^c = S_1^c \quad (4.25)$$

$$S_3^c = S_1^c + \tau_{\max}^c \frac{\tau_f - S_1^2 (\tau_f - \tau_{\max}) - 2\tau_{\max}}{S_1 \tau_{\max} (\tau_f - \tau_{\max})} \quad (4.26)$$

where the residual bond strength τ_f and bond strength τ_{\max} for reinforcement without corrosion are defined by the Eqs. (4.14) to (4.16), respectively, and the parameter S_1 is given by Eq. (4.16).

4.4 Finite element modelling of debonding

A crucial step in the modelling debonding between concrete and reinforcing bars is the representation of bond between concrete and steel bars. Herein, the reinforcing steel is modelled with two noded truss elements, while the concrete is modelled with eight noded hexahedral elements. If complete continuity between finite elements representing concrete and steel bars, bond failure is excluded. To model debonding, the nodal degrees of freedom of the associated elements are not directly coupled but are connected via so-called interface elements. These interface elements are, in effect, nonlinear springs whose force-displacement characteristics are defined as function of the relative sliding or slip between the concrete and the reinforcing bars. The force in the spring can then be expressed as a function of the slip S , that is

$$F(S) = \frac{n}{2} \left(\frac{\pi \emptyset_s}{2} L_e \right) \tau(S) \quad (4.27)$$

where \emptyset_s is the diameter of the reinforcing bars, $\tau(S)$ is the bond stress described in Section 4.3. The concrete beam is reinforced with n reinforcing bars as shown in Figure 4.3. The rein-

forcing steel is modelled with truss elements and L_e is the length of each truss element as shown in Figure 4.3.

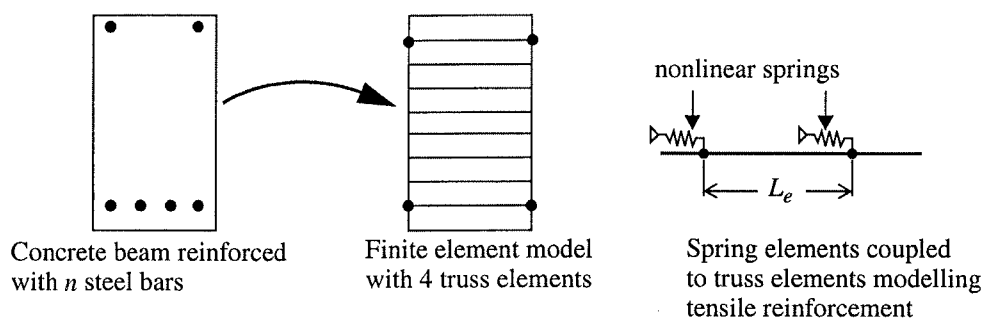


Figure 4.3 Finite element modelling of tensile reinforcement in concrete beam.

When corrosion takes place, this leads to loss of the cross section area of the reinforcing and reduction of the bond strength between concrete and steel bars. To achieve this, the rebars were modelled with two sets of truss elements, labelled as A_1 and A_2 . Truss element set A_1 models the remaining cross section area of the reinforcing bars after corrosion and truss element set A_2 models the cross section loss due to corrosion. The truss element set A_1 is connected to the nodes on the concrete with nonlinear springs labelled as K_1 which models the remaining bond strength after corrosion. Before corrosion takes place, the truss element set A_2 are connected to the nodes on the concrete with the nonlinear springs K_2 via nonlinear couplings. After corrosion takes place, the couplings between the truss element set A_2 and the springs K_2 are removed. Consequently, loss of cross section area and reduced bond strength is achieved.

5. NUMERICAL EXAMPLES

5.1 Deteriorated and repaired beams attacked by uniform corrosion

To illustrate the application of the present approach, the simply supported beam shown in 5.1 was selected. A simply supported beam with a free span of $L = 8.0$ m was subjected to a permanent load $g = 23.75$ kN/m plus a variable load $p = 8$ kN/m. Using Norwegian codes, the beam was designed to sustain an ultimate limit load of 41.3 kN/m. The cross section of the beam is shown in Figure 5.2. In addition to the longitudinal reinforcement, the beam had stirrups of 10 mm diameter and at 500 mm spacing. Uniaxial concrete strengths were 16.0 MPa in compression and 1.21 MPa in tension, after adjustment with material safety factors. Yield strength and elasticity modulus of the reinforcing steel were taken as 400 MPa and 210 GPa, respectively.

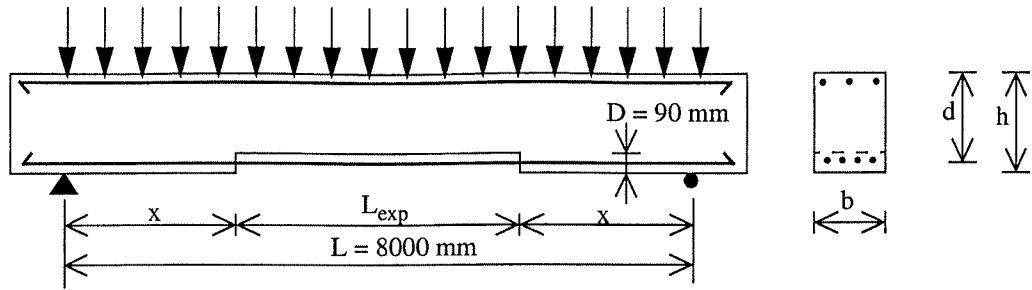


Figure 5.1 Deteriorated and repaired beam.

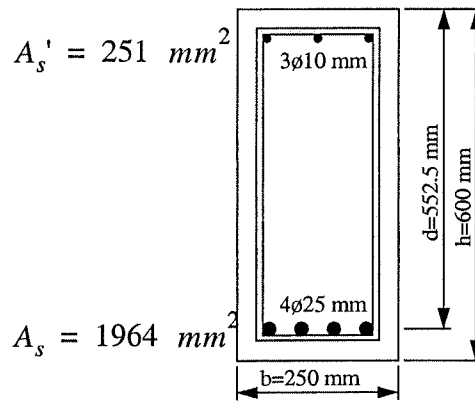


Figure 5.2 Beam cross section.

The concrete beam was modelled with a total of 363 eight noded hexahedral elements and the resulting element mesh is shown in Figure 5.3. Bond slip was modelled as described in Section 4.4 and the bond stress-slip model proposed in CEB-FIP [5] and modified by Tørlien et al. [7] was employed. Bond strength was calculated according to Norwegian code NS3473 [8] and the bond strength τ_f in the uncorroded area of the beam was set equal to 1.17 MPa and bond strength of the corroded rebars of the beam was $\tau_f^c = \tau_f/2$. The Data used in the bond stress-slip models are summarized in Table 5.1.

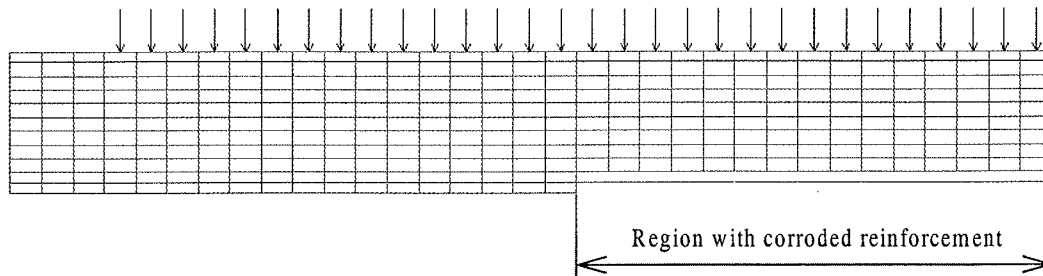


Figure 5.3 Finite element mesh of beam with uniform corrosion.

The numerical analyses were designed to simulate the complete sequence of deterioration and repair identical to that described in Section 2. In addition, the exposed length L_{exp} of the tensile reinforcement was varied as was the degree of corrosion attack.

Table 5.1 Data for bond stress-slip model proposed in CEB-FIP [5] and modified by Tørle et al. [7].

Bond stress-slip model	Re-duction of A_s [%]	τ_{max}	τ_f	λ	S_1^c	S_2^c	S_3^c	α
		or τ_{max}^c [MPa]	or τ_f^c [MPa]		or S_1 [mm]	or S_2 [mm]	or S_3 [mm]	
CEB-FIP/Tørle et al. [7] ¹	10 -25	0.585	0.088	0.073	0.044	0.044	0.07	0.4
CEB-FIP [5] ²	0	1.17	0.176	0.146	0.088	0.088	0.146	0.4

1) Bond strength $\tau_f^c = \tau_f/2$ where $\tau_f = 1, 17$ MPa.
 2) Bond strength τ_f is calculated according to Norwegian code NS3473 [8].

Figures 5.4 and 5.5 shows the calculated force vs. central deflection curves for beams where the cross section area of the tensile reinforcement has been reduced by 10% and 25%, respectively. In addition, the exposed length L_{exp} during the repair phase were selected in the range between 50% to 70% of the span L of the beam. The deteriorated and repaired beams are labelled as “B1T- $\beta\%$ U - αL ”. Here, the values substituted by italic letter a denotes the ratio of exposed length L_{exp} to span L of the beam and the italic letter b denotes the level of corrosion in percent of the cross section of total tensile reinforcement of beams. In the purpose of comparison, finite element simulation of a sound beam was carried with the bond stress-slip model specified in CEB-FIP model code and the calculated force vs. central deflection curve (labelled as B1CEB-FIP-S) is also shown in Figures 5.4 and 5.5.

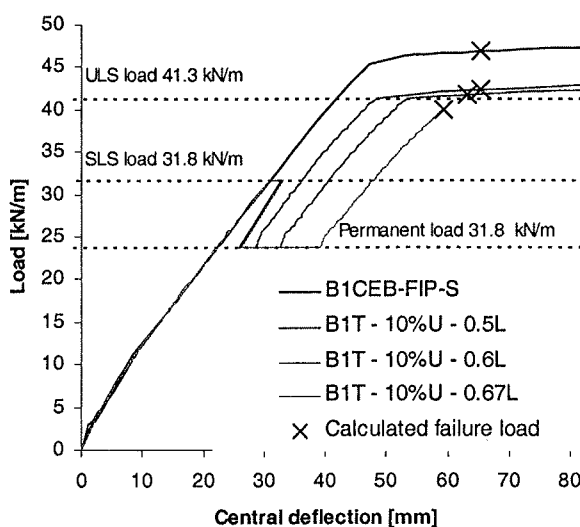


Figure 5.4 Calculated load vs. central deflection curves. Cross section area of tensile reinforcement of the deteriorated and repaired beams has been reduced by 10%.

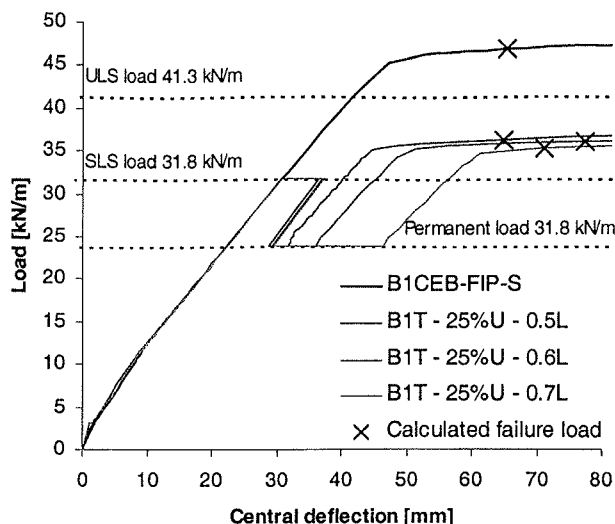


Figure 5.5 Calculated load vs. central deflection curves. Cross section area of tensile reinforcement of the deteriorated and repaired beams has been reduced by 25%.

The calculated failure loads and corresponding central deflections are summarized in Table 5.2 for the sound beam and deteriorated and repaired beams.

Table 5.2 Numerical results obtained from finite element analysis of deteriorated and repaired beams compared with results from a sound beam.

Beam notation	Exposed length L_{exp} [mm]	Reduction of cross section of reinforcement [%]	Central deflection [mm]	Calculated failure load [kN]	Calculated relative failure load [-]	Calculated vs. ULS load	Failure mode*
B1CEB-FIP-S	Sound	0	65.4	46.8	1.00	1,13	C
B1T - 10%U - 0.5L	4000	10	65.5	42.4	0.91	1,03	C
B1T - 10%U - 0.6L	4800	10	63.2	41.8	0.89	1,01	C
B1T - 10%U - 0.67L	5360	10	59.3	40.0	0.86	0,97	D
B1T - 25%U - 0.5L	4000	25	65.0	36.3	0.78	0,88	C
B1T - 25%U - 0.6L	4800	25	77.5	36.1	0.77	0,87	C
B1T - 25%U - 0.7L	5600	25	71.1	35.3	0.75	0,85	C

* D: Debonding, C: Crushing of concrete ($\epsilon_{c,max} > -3.5 \text{ ‰}$), Y/R: Yielding or rupture of reinforcing steel ($\epsilon_{s,max} > 10.0 \text{ ‰}$)

Here, the ULS load 41.3 kN/m as given by Norwegian codes of an undamaged beam was taken as a reference failure load. These simulations demonstrates that the calculated ultimate load for the sound beam is 46.8 kN/m, which is greater then the ULS load 41.3 kN/m. It is seen from Table 5.2 that increasing the exposed length L_{exp} of the tensile reinforcement leads to a reduction of the failure load. Figure 5.4 shows that for beams where the cross sectional area of the tensile reinforcement has been reduced by 10% and the exposed length L_{exp} is smaller then 60% of the span L of the beam, the finite element simulations predicts from 1% to

3% higher failure loads than the ULS load of 41.3 kN/m. As the exposed length L_{exp} was increased to 67%, the calculated failure load was 3% lower than the calculated ULS load of 41.3 MPa. This is due to the change in failure mode from a crushing type of failure to debonding when the exposed length was increased from 60% to 67% of the span of the beam.

The results summarized in Table 5.2 shows that for beams where the cross section area of the tensile reinforcement have been reduced by 25%, the calculated ultimate loads are 12% to 15% lower than the ULS load 41.3 kN/m, but greater than the SLS load of 31.75 kN/m.

Figures 5.6 to 5.7 shows the variation of the calculated slip between the concrete and the rebars along the length of the beams at the predicted failure load.

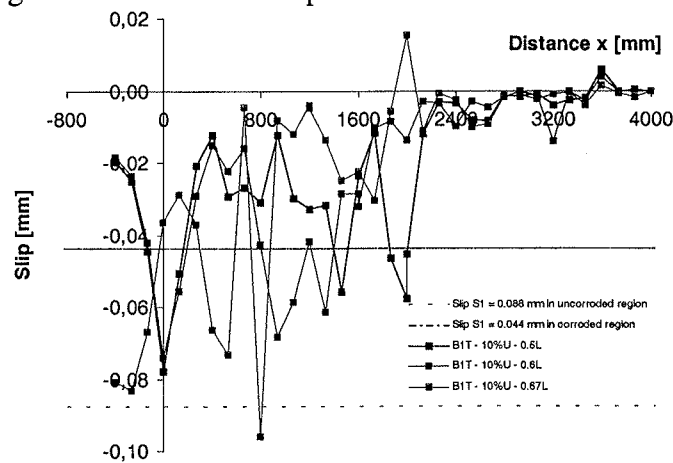


Figure 5.6 Variation of the calculated slip along the length of the beams, cross section area of rebars reduced by 10% due to corrosion. Slip model proposed by CEB-FIP and modified by Tørle [7] with $S_1 = 0.088$ mm in uncorroded region and $S_1 = 0.044$ mm in corroded region of the beams.

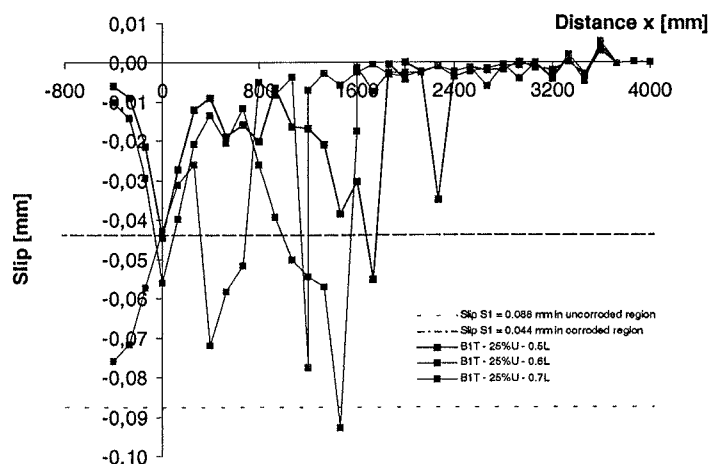


Figure 5.7 Variation of the calculated slip along the length of the beams, cross section area of rebars reduced by 25% due to corrosion. Slip model proposed by CEB-FIP and modified by Tørle [7] with $S_1 = 0.088$ mm in uncorroded region and $S_1 = 0.044$ mm in corroded region of the beams.

Figures 5.8 and 5.9 shows the variation of the calculated slip along the length of the beams labelled as B1T-10%U-0.67L and B1T-10%U-0.7, respectively. The slip between the concrete and rebars are presented at different load levels according to complete sequence of deterioration and repair identical to that described in Section 2 and the letters a-f refers to the different stages in the deterioration and repair history as illustrated in Figures 2.1 and 2.2. It is seen from Figures 5.8 and 5.9 that debonding starts after application of repair mortar (see Figure 2.1f) at the end of the repaired zone of the concrete beam. Further loading leads to propagation of bond failure towards the supports.

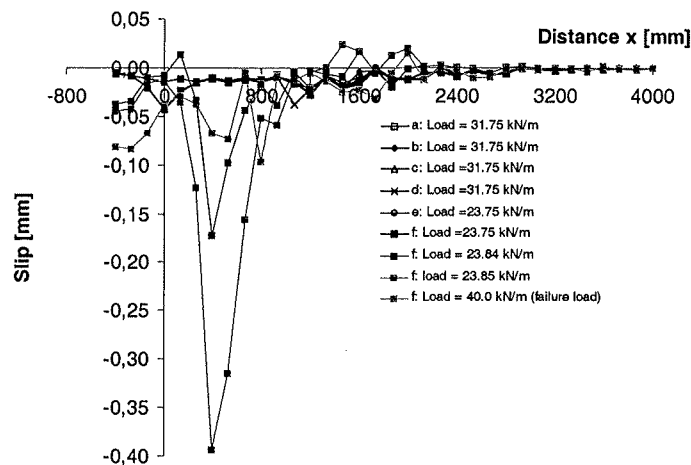


Figure 5.8 Variation of the calculated slip along the length of the beam labelled as B1T-10%U-0.67L at different load levels. $S_1 = 0.088$ mm in uncorroded region and $S_1 = 0.044$ mm in corroded region of the beams.

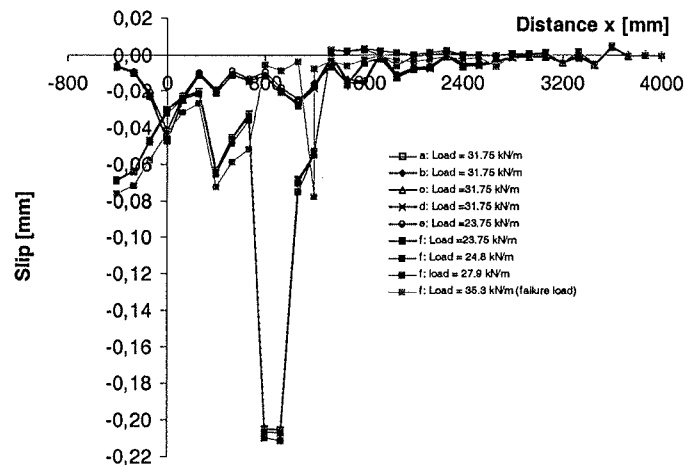


Figure 5.9 Variation of the calculated slip along the length of the beam labelled as B1T-25%U-0.7L at different load levels. $S_1 = 0.088$ mm in uncorroded region and $S_1 = 0.044$ mm in corroded region of the beams.

To study the effect of varying the bond strength on the calculated failure load, the bond strength τ_f in the uncorroded region of the beams was calculated according CEB-FIP [5] and the resulting bond strength was 1.68 MPa. Again, the bond stress-slip model proposed in CEB-FIP [5] and modified by Tørle et al. [7] was applied to model bond slip in the corroded

region of the beam and the bond strength between the concrete and the corroded rebars was selected as $\tau_f^c = \tau_f/2$. Finite element simulations of deteriorated and repaired beams were also carried out based on the bond stress-slip model proposed in CEB-FIP [5] and modified by Castellani et al. [6] as described in 4.3. The bond strength between the concrete and the corroded rebars was estimated using the empirical formula by Rodriguez et al. [4], see Eq. (4.8). The resulting value for the deteriorated bond strength τ_{max}^c was 1.31 MPa and 1.37 MPa when the cross section loss due to corrosion of the tensile rebars were selected as 10% and 25%, respectively. The data used in the bond stress-slip models are given in Table 5.3.

Nonlinear finite element analysis of repaired and deteriorated beams were carried out by using the element mesh shown Figure 5.3 and the beam were subjected to the sequence of deterioration and repair identical to that described in described in Section 2, Figure 2.1. In these finite element simulations, the tensile reinforcement of the beams have been reduced by 10% and 25%, respectively. In addition, the exposed length L_{exp} were selected in the range between 50% to 70% of the span L of the beams.

Table 5.3 Data for bond stress-slip model proposed in CEB-FIP [5] and modified by Tørhlen et al. [7] or Castellani et al. [6].

Bond stress-slip model	Red. of A_s [%]	τ_{max} or τ_{max}^c [MPa]	τ_f or τ_f^c [MPa]	λ	S_1^c or S_1 [mm]	S_2^c or S_2 [mm]	S_3^c or S_3 [mm]	α
CEB-FIP/Castellani et al. [6] ¹	25	1.31	0	-	0,066	0,067	0,146	0.4
CEB-FIP/Castellani et al. [6] ¹	10	1.37	0	-	0.076	0.077	0.155	0.4
CEB-FIP/Tørhlen et al. [7] ¹	10 -25	0.84	0.126	0.105	0.063	0.063	0.011	0.4
CEB-FIP [5] ²	0	1.68	0.252	0.210	0.126	0.126	0.210	0.4

1) Bond strength $\tau_f^c = \tau_f/2$ where $\tau_f = 1,68$ MPa and it is calculated according model code 1990 [5].
2) Bond strength τ_f calculated according to model code 1990 [5].

The results obtained from the finite element simulations are summarized in Table 5.4 Here, the analyses based on the slip model proposed in CEB-FIP and modified by Tørhlen et al. are labelled as “BIT- $\beta\%U$ - αL ”, and those based on the slip model proposed in CEB-FIP and modified by Castellani et al. are labelled as “B1C- $b\%U$ - bL ”. Here, the values substituted by italic letter a denotes the ratio of exposed length L_{exp} to span L of the beam and the italic letter b denotes the level of corrosion in percent of the cross section of total tensile reinforcement of beams.

In the purpose of comparison, calculated force vs. central deflection curve obtained from finite element analysis of the sound beam (labelled as B1CEB-FIP-S) is also shown in the Figures 5.10 and 5.11. It is seen from Table 5.4 that if the corrosion level and the length L_{exp} are identical, the two different slip models predicts approximately the same failure load and the deviations may be due to numerical effects. But, the slip model proposed in CEB-FIP and modified by Tørlien et al. produced somewhat larger central deflections of the beams compared with those obtained by using the slip model proposed in CEB-FIP and modified by Castellani et al..

Table 5.4 Numerical results obtained from finite element analysis of deteriorated and repaired beams compared with results from a sound undamaged beam.

Beam notation	Bond stress-slip model	Exposed length L_{exp} [mm]	Reduction of cross section of reinforcement [%]	Central deflection [mm]	Calculated failure load [kN]	Calculated relative failure load [-]	Calculated vs. ULS load	Failure mode*
B1CEB-FIP-S	C	Sound	0	65,4	46,8	1,00	1,13	C
B1T-10%U-0.5L	C/T	4000	10	63.6	42.3	0.90	1.03	C
B1T-10%U-0.6L	C/T	4800	10	70.5	42.0	0.90	1.02	C
B1T-10%U-0.7L	C/T	5600	10	70.5	41.6	0.89	1.01	C
B1T-25%U-0.5L	C/T	4000	25	79.5	36.7	0.78	0.89	C
B1T-25%U-0.6L	C/T	4800	25	75.1	36.1	0.77	0.87	C
B1T-25%U-0.7L	C/T	5600	25	71.8	35.6	0.76	0.86	C
B1C-10%U-0.5L	C/C	4000	10	63.0	42.3	0.90	1.03	C
B1C-0%U-0.6L	C/C	4800	10	68.7	42.1	0.90	1.02	C
B1C-10%U-0.7L	C/C	5600	10	65.7	41.3	0.88	1.00	C
B1C-25%U-0.5L	C/C	4000	25	73.5	36.6	0.78	0.89	C
B1C-25%U-0.6L	C/C	4800	25	71.6	36.1	0.77	0.87	C
B1C-25%U-0.7L	C/C	5600	25	70.0	35.5	0.76	0.86	C

* C: CEB-FIP, C/T: CEB-FIP/Tørlien, C/C: CEB-FIP/Castellani
 ** D: Debonding, C: Crushing of concrete ($\epsilon_{c,min} > -3.5 \text{ ‰}$), Y/R: Yielding or rupture of reinforcing steel ($\epsilon_{s,max} > 10.0 \text{ ‰}$), D/C: Debonding and crushing.

Comparisons of the results given in Tables 5.2 and 5.4 demonstrates that by increasing the bond strengths from $\tau_{max}=1.17$ MPa and $\tau_{max}^c=0.59$ MPa to $\tau_{max}=1.68$ MPa and $\tau_{max}^c=0.84$ MPa, the deviations between the calculated failure loads are small, except when the exposed Length L_{exp} tensile reinforcement was 50% of the span L and the tensile reinforcement was reduced by 10% due to uniform corrosion. In this case, the smaller values ($\tau_{max}=1.17$ MPa and $\tau_{max}^c=0.59$ MPa) of the bond strength produced lower failure load compared with that predicted with the higher value of the bond strength ($\tau_{max}=1.68$ MPa and $\tau_{max}^c=0.84$ MPa). This is due to the fact that debonding occurred earlier when the lower values of the bond strength were selected. Comparisons of the calculated central deflections at failure shows some discrepancies, which may be due to numerical effects. Since the load-central deflection curves in most of the cases are approximately horizontal at the load level of failure, only small changes in the predicted values of the failure load may lead to considerable variations in the corre-

sponding central deflections. The the calculated force vs. central deflection curves for the deteriorated and repaired beams are portrayed in Figures 5.10 and 5.11. These simulations demonstrate that for beams where the tensile reinforcement has been reduced by 10%, the calculated failure loads are approximately same as the ULS load of 41.3 kN/m, see Figures 5.10a and 5.11a. Further reduction of the cross section of the tensile reinforcement, i.e. 30%, leads to increased central deflections and a considerable reduction of the calculated failure loads, see Figures 5.10b and 5.11b. The calculated failure loads greater then the SLS load of 31.75 kN/m, but only 86% - 89% of the ULS load 41.3 kN/m depending on the exposed length L_{exp} during the repair phase.

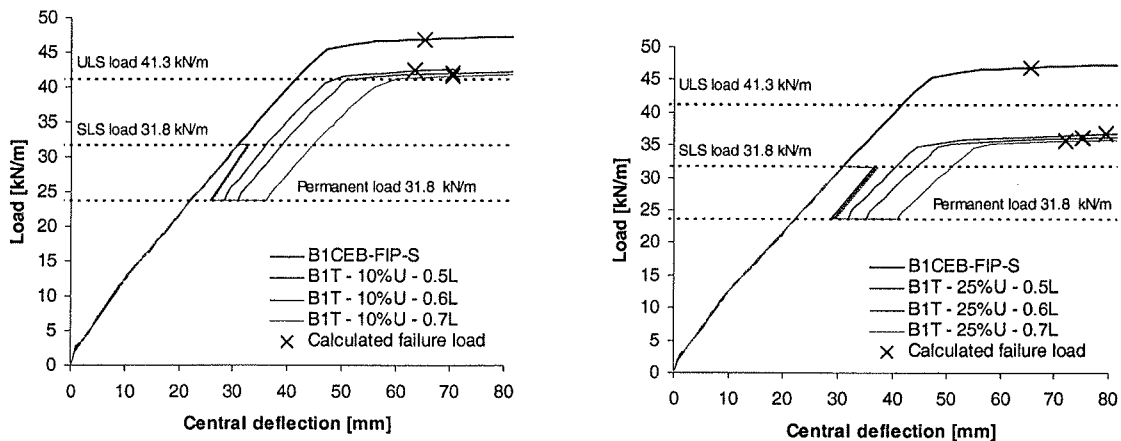


Figure 5.10 Load vs. central deflection curves obtained from finite element analysis based on the slip model proposed by CEB-FIP and modified by Tørleén [7]. a) Cross section area of tensile reinforcement of the deteriorated and repaired beams has been reduced by 0%. b) Cross section area of tensile reinforcement of the deteriorated and repaired beams has been reduced by 25%.

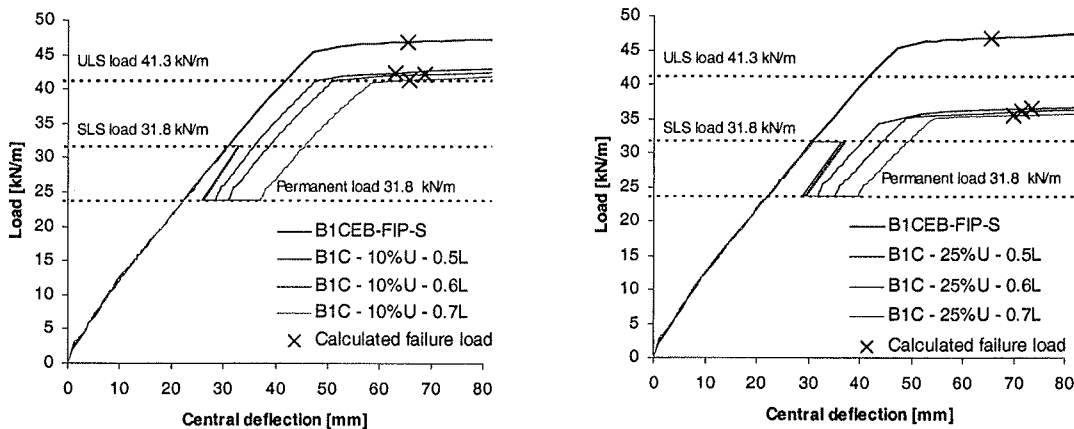


Figure 5.11 Load vs. central deflection curves obtained from finite element analysis based on the slip model proposed by CEB-FIP and modified by Castellani [6]. a) Cross section area of tensile reinforcement of the deteriorated and repaired beams has been reduced by 10%. b) Cross section area of tensile reinforcement of the deteriorated and repaired beams has been reduced by 25%.

Figures 5.12 to 5.15 shows the variation of the calculated slip between the concrete and the rebars along the length of the beams at the predicted failure load.

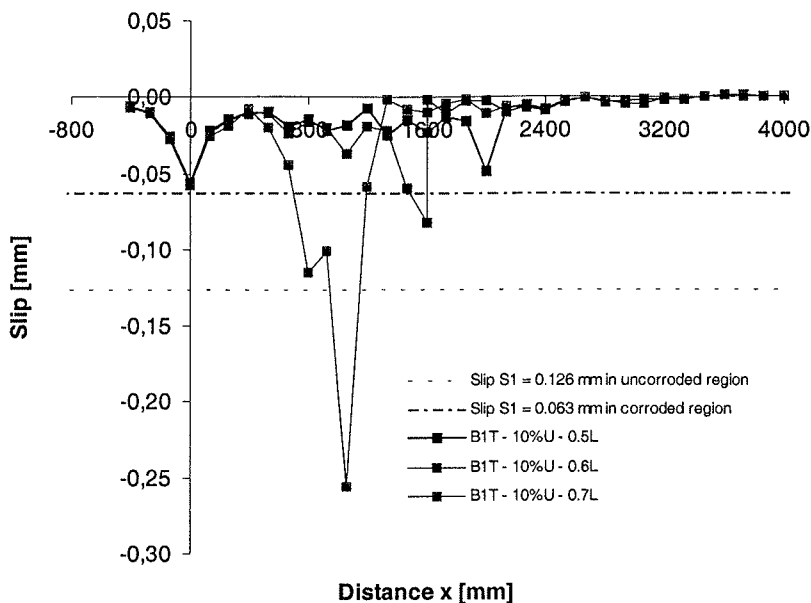


Figure 5.12 Variation of the calculated slip along the length of the beams, cross section area of tensile reinforcement is reduced by 10%. Slip model proposed by CEB-FIP and modified by Tørlelen [7] with $S_1 = 0.126$ mm in uncorroded region and $S_1 = 0.076$ mm in corroded region of the beams.

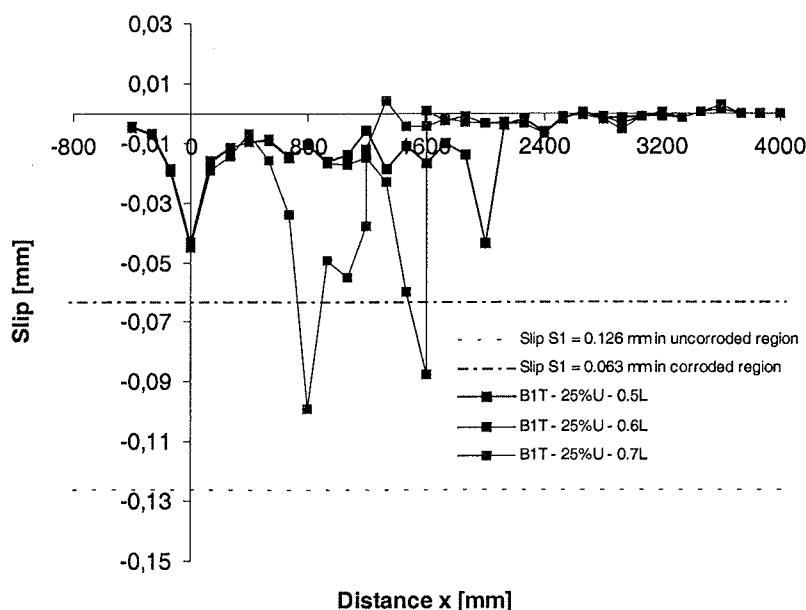


Figure 5.13 Variation of the calculated slip along the length of the beams, cross section area of tensile reinforcement is reduced by 25%. Slip model proposed by CEB-FIP and modified by Tørlelen [7] with $S_1 = 0.126$ mm in uncorroded region and $S_1 = 0.063$ mm in corroded region of the beams.

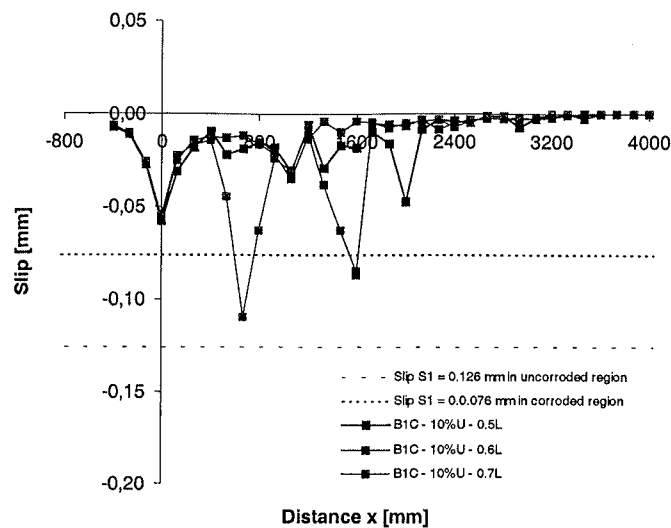


Figure 5.14 Variation of the calculated slip along the length of the beams, cross section area of rebars reduced by 10% due to corrosion. Slip model proposed by CEB-FIP and modified by Castellani [6] $S_1 = 0.126$ mm in uncorroded region and $S_1 = 0.076$ mm in corroded region of the beams.

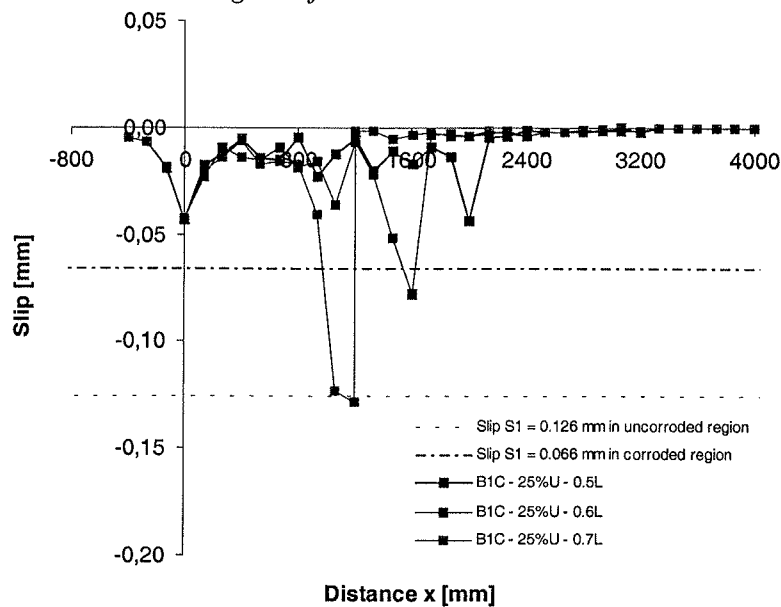


Figure 5.15 Variation of the calculated slip along the length of the beams, cross section area of rebars reduced by 25% due to corrosion. Slip model proposed by CEB-FIP and modified by Castellani [6] $S_1 = 0.126$ mm in uncorroded region and $S_1 = 0.066$ mm in corroded region of the beams.

5.2 Deteriorated and repaired beams attacked by uniform corrosion and pitting

As described in Section 4, corrosion in either carbonated or chloride contaminated concrete reduces the reinforcing bar section. Whereas uniform or homogenous attack penetration at the bars occurs in carbonated concrete, chlorides may produce localized attack often referred to as

pitting and cause a significant section decrease. If the tensile reinforcement in a beam is attacked by uniform corrosion, the residual cross section area of the tensile reinforcement can be estimated from Eq. (4.5), while the residual cross section area can be estimated from Eq. (4.6) when the reinforcement is attacked by pitting and uniform corrosion. In Eq. (4.6) it is assumed that only one rebar is attacked by pitting and the remaining rebars are attacked by uniform corrosion.

To investigate the effect of pitting corrosion a concrete beam with the dimensions shown in Figure 5.1 was modelled with a total of 363 eight noded hexahedral elements and the resulting element mesh is shown in Figure 5.16. and the bond stress-slip model proposed in CEB-FIP [5] and modified by Castellani et al. [6] was employed and the data used in the bond model are given in Table 5.5. Herein, the compressive and tensile reinforcement are modelled with truss elements as described in Section 4.4. Pitting of the tensile reinforcement is introduced by reducing the cross section area of truss elements at the cross section of the center of the beam as shown in Figure 5.16. To avoid twisting of the beam, the reduction in cross section area due to pitting of tensile reinforcement is equally distributed in the reinforcement on both sides of the beam.

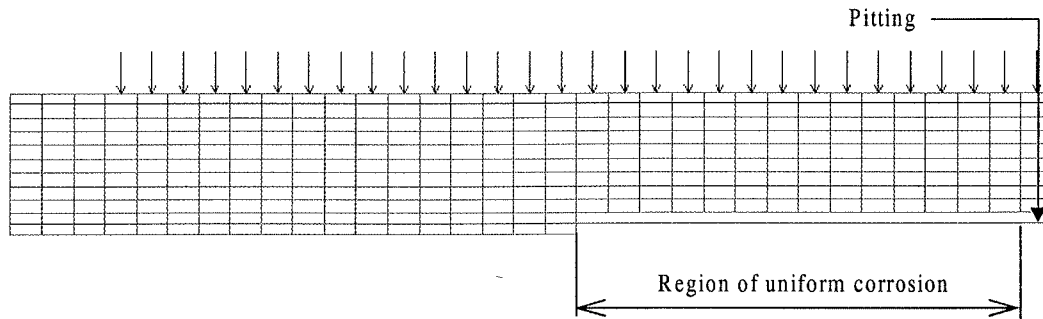


Figure 5.16 Finite element mesh of beam attacked by uniform corrosion and pitting.

Table 5.5 Data for bond stress-slip model proposed in CEB-FIP [5] and modified by Tørle et al. [7] or Castellani et al. [6].

Bond stress-slip model	τ_{max}	τ_f	λ	S_1^c	S_2^c	S_3^c	α
	or τ_{max}^c [MPa]	or τ_f^c [MPa]		or S_1 [mm]	or S_2 [mm]	or S_3 [mm]	
CEB-FIP/Castellani et al. [6] ¹	1.31	0	-	0,066	0,067	0,146	0.4
CEB-FIP [5] ²	1.68	0.252	0.210	0.126	0.126	0.210	0.4

1) Bond strength $\tau_f^c = \tau_f/2$ where $\tau_f = 1,68$ MPa and it is calculated according model code 1990 [5].
 2) Bond strength τ_f calculated according to model code 1990 [5].

Figure 5.17 shows the calculated load versus central deflection curves obtained by finite element simulation of the complete deterioration- and repair history of the beams. Here, the tensile reinforcement of the repaired beams have been exposed 50% of the span of the beams and the cross section area of the tensile reinforcement is reduced by 25% due to uniform corrosion over the exposed length of the beam and 38% due to pitting at the center of the beam. The beam exposed to uniform corrosion and pitting is here labelled as B1-25%U+38%P-0.5L. In the purpose of comparison, the calculated load versus central deflection curves obtained from finite element simulation of a sound beam and a beam attacked only uniform corrosion are also shown in Figure 5.17.

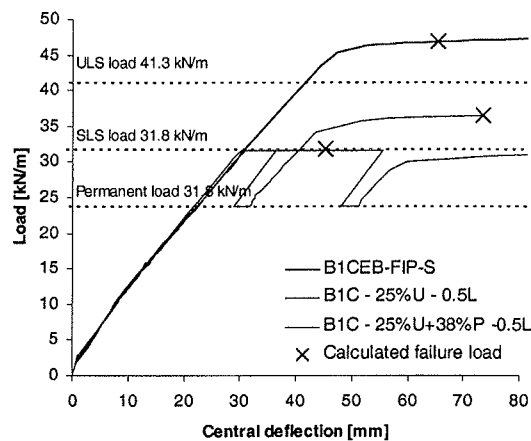


Figure 5.17 Load vs. central deflection curves obtained from finite element analysis based on the slip model proposed by CEB-FIP and modified by Castellani [6].

The results from the finite element simulations are summarized in Table 5.6 which shows that for a beam where the cross section area of the tensile reinforcement has been reduced by 25% due to uniform corrosion and 38% due to pitting, the calculated limit load is equal to the SLS load of 31.8 kN/m, which is only 77% of the ULS load of 41.3 kN/m. Moreover, it is seen from Table 5.6 that reducing the cross section of the tensile reinforcement by 38% due to pitting leads to decreased deflection at failure.

Table 5.6 Numerical results obtained from finite element analysis of deteriorated and repaired beams compared with results from a sound undamaged beam.

Beam notation	Exposed length L_{exp} [mm]	Reduction of cross section of reinforcement [%]	Central deflection [mm]	Calculated failure load [kN]	Calculated relative failure load [-]	Calculated vs. ULS load	Failure mode*
B1CEB-FIP-S	Sound	0	65,4	46,8	1,00	1,13	C
B1C - 25%U-0.5L	4000	25	79.5	36.7	0.78	0.89	C
B1C - 25%U+38%P-0.5L	4000	25 and 38	45.3	31.8	0.68	0.77	Y/R

* D: Debonding, C: Crushing of concrete ($\epsilon_{c,min} > -3.5 \cdot 10^{-3}$), Y/R: Yielding or rupture of reinforcing steel ($\epsilon_{s,max} > 10.0 \cdot 10^{-3}$), D/C: Debonding and crushing.

This is due to yielding and rupture in the pit on the tensile reinforcement at the centre of the beam. The calculated compressive strain in the concrete and the tensile strain in pit on the tensile reinforcement at the centre of the beam and is plotted versus the central deflection of the beam in Figure 5.18.

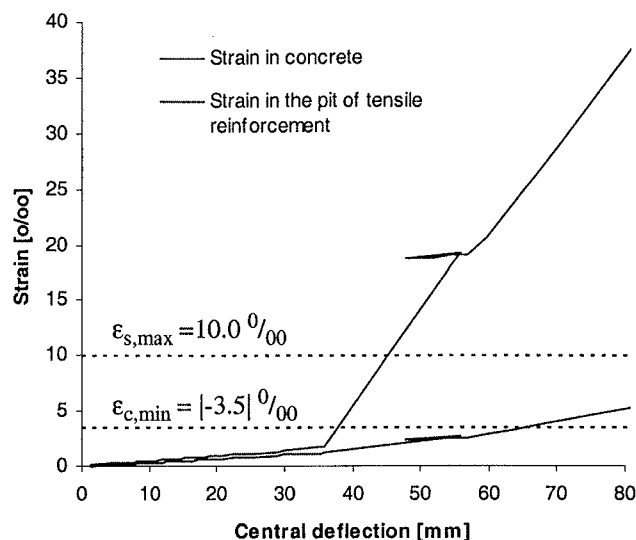


Figure 5.18 Strain in concrete and in the pit of the tensile reinforcement vs. central deflection obtained from finite element analysis of a beam with where the cross section area of the tensile reinforcement has been reduced by 25% due to corrosion and 38% due to pitting.

Here, rupture of the reinforcing steel is defined when the maximum strain in the steel exceeds $10.0‰$, and crushing of concrete is defined to occur when the compressive strains in the concrete exceeds $3.5‰$. From Figure 5.18 it is seen that rupture of the tensile reinforcement occurred when the central deflection of the beam was 45.3 mm.

5.3 Deteriorated and repaired beams with spliced reinforcement attacked by uniform corrosion

To investigate the effect of splicing the tensile reinforcement on the calculated failure load, the same type of beams as analysed in the previous sections were considered, except that the tensile reinforcement was spliced. By using Norwegian codes, the beam was designed to sustain the ultimate limit load of 41.3 kN/m. The cross section of the beam is shown in Figure 5.2. In addition to the spliced longitudinal reinforcement, the beam had stirrups of 10 mm diameter and at 500 mm spacing. Uniaxial concrete strengths were 16.0 MPa in compression and 1.21 MPa in tension, after adjustment with material safety factors. Yield strength and elasticity modulus of the reinforcing steel were taken as 400 MPa and 210 GPa, respectively.

The concrete beam was modelled with a total of 363 eight noded hexahedral elements and the resulting element mesh is shown in Figure 5.3. Bond slip was modelled as described in Sec-

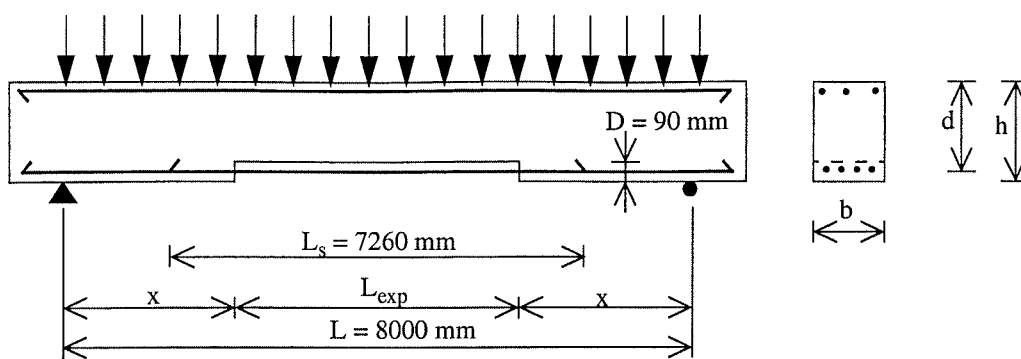


Figure 5.19 Deteriorated and repaired beam with spliced tensile reinforcement.

tion 4.4 and the bond stress-slip model proposed in CEB-FIP [5] and modified by Castellani et al. [6] was employed. The bond strength between the concrete and the corroded rebars was estimated using the empirical formula by Rodriguez et al. [4], see Eq. (4.8). The resulting values for the deteriorated bond strength τ_{max}^c was 1.31 MPa and 1.37 MPa when the reduction of the cross section of the tensile reinforcement were selected as 10% and 25%, respectively. The data used in the bond stress-slip models are given in Table 5.3.

Nonlinear finite element analysis of sound and repaired and deteriorated beams were carried out by using the element mesh shown Figure 5.20. Here the concrete was modelled with a total of 363 eight noded hexahedral elements and the compressive and tensile reinforcement reinforcement are modelled with truss elements as described in Section 4.4.

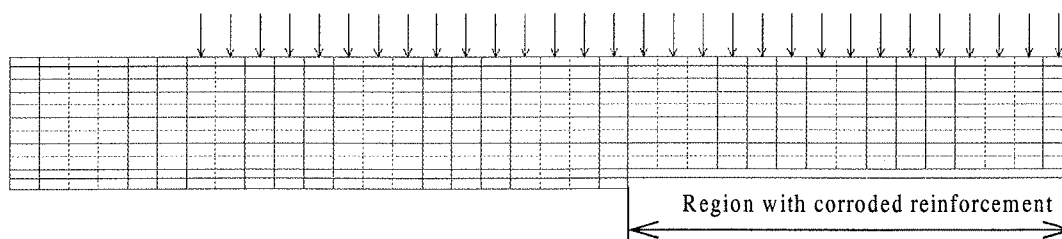


Figure 5.20 Finite element mesh of beam with spliced tensile reinforcement attacked by uniform corrosion.

In the finite element simulations of the complete repair and deterioration history of the beams, the tensile reinforcement of the beams have been reduced by 10% and 25% due to uniform corrosion. In addition, the exposed length L_{exp} were selected in the range between 50% to 70% of the span L of the beams during the repair phase. Figure 5.21 shows the calculated load versus central deflection curves for deteriorated and repaired beams. These beams are labelled as “B2C-*b*%U -*b*L”. Here, the values substituted by italic letter *a* denotes the ratio of exposed

length L_{exp} to span L of the beam and the italic letter b denotes the level of corrosion in percent of the cross section of total tensile reinforcement of beams. In the purpose of comparison, finite element simulation of a sound beam was carried with the bond stress-slip model specified in CEB-FIP model code. The calculated force vs. central deflection curve (labelled as B2CEB-FIP-S) is also shown in Figure 5.21.

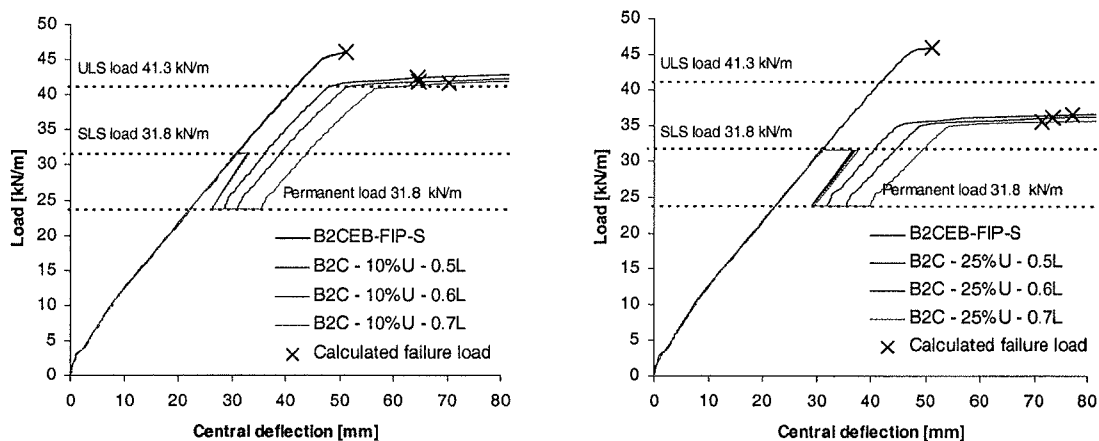


Figure 5.21 Load vs. central deflection curves obtained from finite element analysis based on the slip model proposed by CEB-FIP and modified by Castellani [6]. a) Cross section area of tensile reinforcement of the deteriorated and repaired beams has been reduced by 10%. b) Cross section area of tensile reinforcement of the deteriorated and repaired beams has been reduced by 25%.

The calculated failure loads and corresponding central deflections are summarized in Table 5.7 for the sound beams and deteriorated and repaired beams.

Table 5.7 Numerical results obtained from finite element analysis of deteriorated and repaired beams compared with results from a sound undamaged beam.

Beam notation	Exposed length L_{exp} [mm]	Reduction of cross section of reinforcement [%]	Central deflection [mm]	Calculated failure load [kN]	Calculated relative failure load [-]	Calculated vs. ULS load	Failure mode* *
B2CEB-FIP-S	Sound	0	51,1	46,0	1,00	1,11	D
B2C-10%U-0.5L	4000	10	64,4	42,3	0,92	1,03	C
B2C-10%U-0.6L	4800	10	64,8	41,8	0,91	1,01	C
B2C-10%U-0.7L	5600	10	70,5	41,6	0,90	1,01	C
B2C-25%U-0.5L	4000	25	77,1	36,6	0,80	0,89	C
B2C-25%U-0.6L	4800	25	73,5	36,1	0,78	0,87	C
B2C-25%U-0.7L	5600	25	71,5	35,5	0,77	0,86	C

* C: CEB-FIP, C/T: CEB-FIP/Tørnlen, C/C: CEB-FIP/Castellani
 ** D: Debonding, C: Crushing of concrete ($\epsilon_{c,min} > -3.5 \text{‰}$), Y/R: Yielding or rupture of reinforcing steel ($\epsilon_{s,max} > 10.0 \text{‰}$)

It is seen from the table above that the calculated ultimate load of sound beam is 46.0 kN/m, which is 11% greater than the ULS load of 41.3 kN/m. For the beams with 10% reduction of

the tensile reinforcement, the ultimate load decreases from 3% to 1% greater than the ULS load of 41.3 kN/m as the exposed length L_{exp} during the repair phase increases from 50% to 70% of the span width L . When the tensile reinforcement is reduced by 25% due to uniform corrosion, the calculated failure loads decrease from 80% to 77% of the ULS load as the exposed length L_{exp} increases from 50% to 70% during the repair phase.

Figures 5.22 and 5.23 show the variation of the calculated slip between the concrete and the rebars along the length of the beams at the predicted failure load.

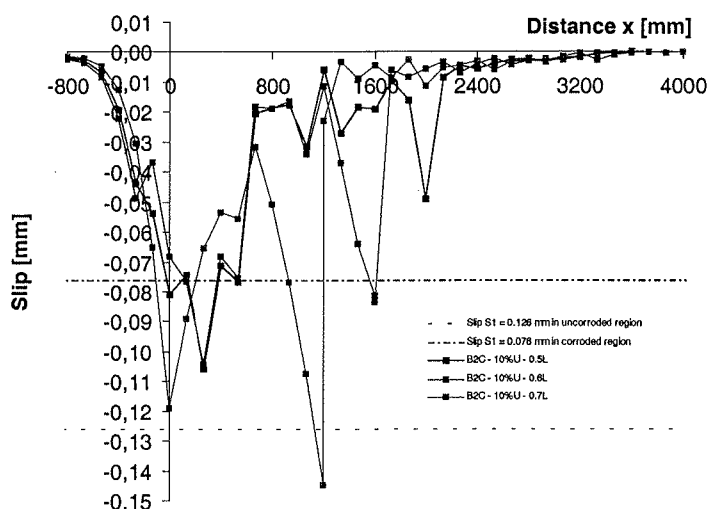


Figure 5.22 Variation of the calculated slip along the length of the beams, cross section area of tensile reinforcement is reduced by 10%. Slip model proposed by CEB-FIP and modified by Tørle [7] with $S_1 = 0.126$ mm in uncorroded region and $S_1 = 0.076$ mm in corroded region of the beams.

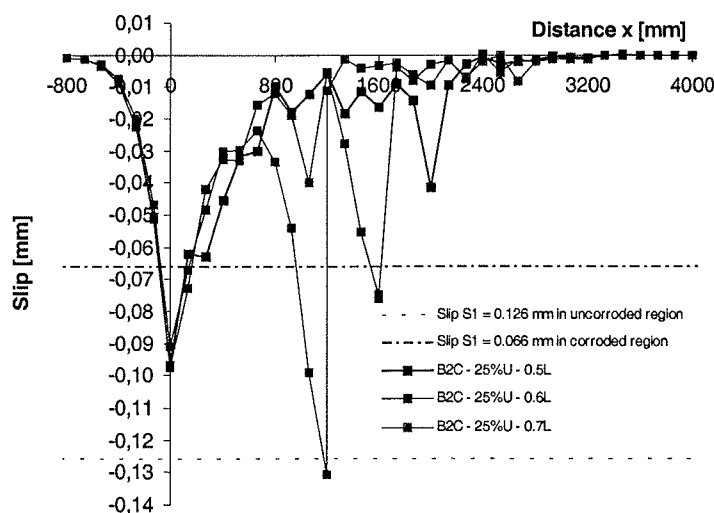


Figure 5.23 Variation of the calculated slip along the length of the beams, cross section area of tensile reinforcement is reduced by 25%. Slip model proposed by CEB-FIP and modified by Tørle [7] with $S_1 = 0.126$ mm in uncorroded region and $S_1 = 0.063$ mm in corroded region of the beams.

5.4 Deteriorated and repaired beams with spliced reinforcement attacked by uniform corrosion and pitting

To study effects of pitting corrosion on RC beams with spliced reinforcement, the beam shown in Figure 5.19 was considered. The concrete beam was discretized with a total 363 hexahedral elements, as shown in Figure 5.24. The bond stress-slip model proposed in CEB-FIP and modified by Castellani et al. [6] was applied and the data used in the bond model are given in Table 5.3. The compressive and tensile reinforcement are modelled with truss elements as described in Section 4.4, and pitting of the tensile reinforcement was introduced as described in Section 5.2.

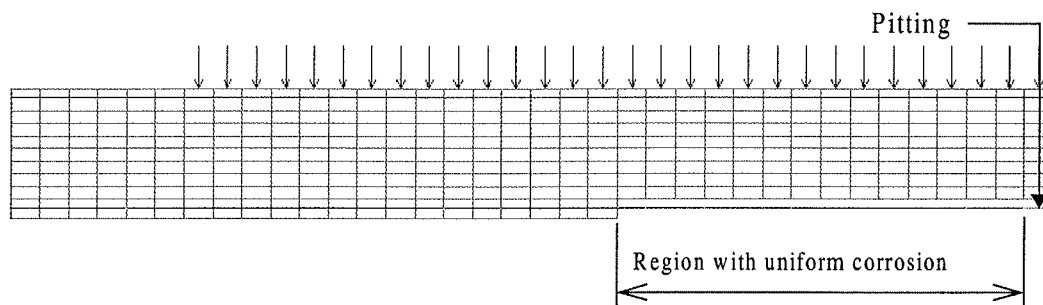


Figure 5.24 Finite element mesh of beam with spliced tensile reinforcement attacked by uniform corrosion and pitting.

Figure 5.25 shows the load versus central deflection curve obtained from finite element simulations of the complete deterioration and repair history of the beam.

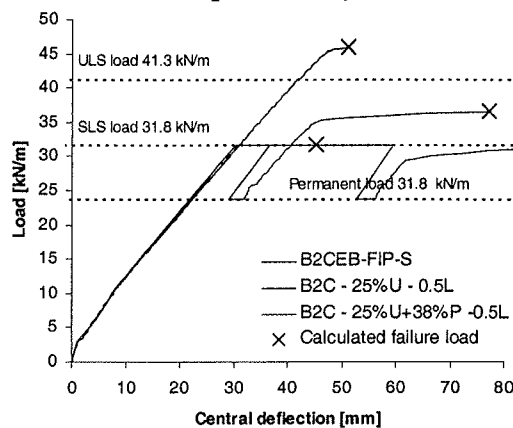


Figure 5.25 Load vs. central deflection curves obtained from finite element analysis based on the slip model proposed by CEB-FIP and modified by Castellani [6].

The cross section of the area of the tensile reinforcement was reduced by 25% due to uniform corrosion over the exposed length L_{exp} equal to 50% of the span L of the beam. In addition, the tensile reinforcement was reduced by 38% due to pitting corrosion. The pit was located at the centre of the beam as shown in Figure 5.24. The beam attacked by uniform corrosion and pitting is labelled as B2-25%U+38%P-0.5L. In the purpose of comparison, the calculated load versus central deflection curves of a sound beam and a beam attacked by only uniform corro-

sion are also shown in Figure 5.25. The sound beam and the deteriorated and repaired beam are labelled as B2CEB-FIP-S and B2C-25%U-0.5L, respectively. The results from the finite element simulations are summarized in Table 5.8 which shows that for a beam where the cross section area of the tensile reinforcement has been reduced by 25% due to uniform corrosion and 38% due to pitting, the calculated limit load is equal to the SLS load of 31.8 kN/m, which is only 77% of the ULS load of 41.3 kN/m. Moreover, it is seen from Table 5.6 that reducing the cross section of the tensile reinforcement by 38% due to pitting leads to decreased deflection at failure.

Table 5.8 Numerical results obtained from finite element analysis of deteriorated and repaired beams compared with results from a sound undamaged beam.

Beam notation	Exposed length L_{exp} [mm]	Reduction of cross section of reinforcement [%]	Central deflection [mm]	Calculated failure load [kN]	Calculated relative failure load [-]	Calculated vs. ULS load	Failure mode*
B2CEB-FIP-S	Sound	0	65.4	46.8	1.00	1.13	C
B2C-25%U-0.5L	4000	25	77.1	36.6	0.80	0.89	C
B2C-25%U+38%P-0.5L	4000	25 and 38	45.2	31.8	0.69	0.77	Y/R

* D: Debonding, C: Crushing of concrete ($\epsilon_{c,min} > -3.5 \text{‰}$), Y/R: Yielding or rupture of reinforcing steel ($\epsilon_{s,max} > 10.0 \text{‰}$), D/C: Debonding and crushing.

This is due to yielding and rupture in the pit on the tensile reinforcement at the centre of the beam. The calculated compressive strain in the concrete and the tensile strain in pit on the tensile reinforcement at the centre of the beam and is plotted versus the central deflection of the beam in Figure 5.26.

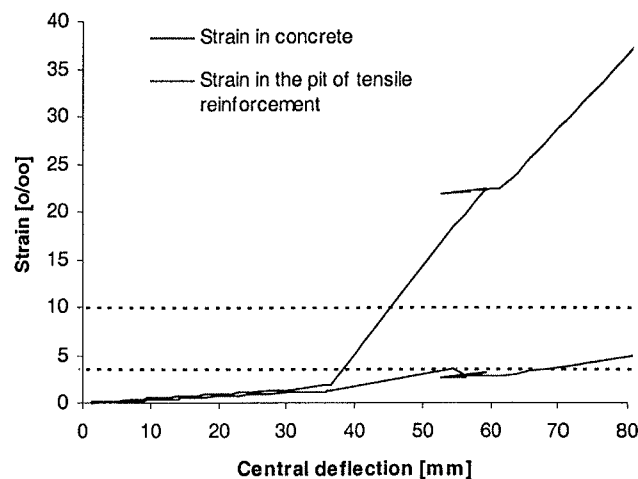


Figure 5.26 Strain in concrete and in the pit of the tensile reinforcement vs. central deflection obtained from finite element analysis of a beam with where the cross section area of the tensile reinforcement has been reduced by 25% due to corrosion and 38% due to pitting.

Here, rupture of the reinforcing steel is defined to occur when the maximum strain in the steel exceeds $10.0‰$, and crushing of concrete is defined to occur when the compressive strains in the concrete exceeds $3.5‰$. From Figure 5.26 it is seen that rupture of the tensile reinforcement occurs when the central deflection of the beam is 45.2 mm.

6. CONCLUDING REMARKS

Corrosion of embedded reinforcement steel due to carbonation chloride ingress continues to pose threats to performance and integrity of reinforced concrete structures. Corrosion attack leads to reduced cross section area of steel bars and reduced bond strength. The associated reductions in stiffness and ultimate strength may be considerable. The removal of chloride contaminated concrete in reinforced concrete structure may also lead to additional loss of stiffness and strength during the repair phase. The structural consequences of these reduced ability to carry load is of great importance for selecting a proper repair procedure. Moreover, conventional mechanical repair procedure may not fully restore the load-carrying capacity. All of this exposes the need for accurate and reliable methods for assessment of residual stiffness and strength of deteriorated and repaired concrete structures. Simple analytical models are of limited value for predicting the complex behavior of concrete structure during the complete deterioration and repair history.

An attempt to solve this problem has been described in the present report, which has focused attention on the use of nonlinear finite element analysis to obtain failure loads of deteriorated and repaired concrete beams. This approach was based on constitutive models for concrete that can realistically represent both compressive crushing and tensile cracking of the material. Plastic yielding of the tensile reinforcement was also taken into account. Particular consideration has been given to the representation of bond between concrete and the embedded reinforcing bars. As uniform corrosion takes place over a given portion of the beams, the reduced cross section area of the tensile reinforcement and reduced bond strength between concrete and the embedded reinforcing bars are also taken into account. A special procedure was employed for simulation of the true loading and straining history of concrete beams subjected to deterioration and corrosion of embedded steel reinforcement, followed by subsequent mechanical repair. The reinforcing rebars were attacked by uniform corrosion or uniform corrosion and pitting. Three different constitutive models were employed to model bond between the embedded rebars and concrete. The shear stress-slip model proposed in CEB-FIP was applied to model bond between uncorroded rebars and concrete, while bond between corroded rebars and concrete was based either on the shear stress-slip model proposed Tørren et al. or on the model proposed by Castellani et al.

Numerical examples in the form of deteriorated and repaired concrete beams with or without spliced tensile reinforcement were presented. Using Norwegian codes, the beam was designed to sustain an ultimate limit load (ULS) of 41.3 kN/m. The cross section tensile reinforcement of deteriorated and repaired beams were reduced by 10% or 25% due to uniform corrosion and the tensile reinforcement were exposed over a length of 50% to 70% of the span of the beams during the repair phase. The finite element simulations demonstrated that the calculated ultimate load decreases as the exposed length and the reduction in cross section area of the tensile reinforcement increases. For beams with 10% reduction of the tensile reinforcement, the calculated ultimate load are from 1% to 3% greater than the ULS load of 41.3 kN/m, while beams with 25% reduction only could sustain a load which were in the range between 86% to 89% of the ULS load. Splicing the tensile reinforcement of the concrete beams had only minor effects on the calculated ultimate load, but some difference in the distribution of the shear stress-slip along the beams were observed. Finite element simulations of deteriorated and repaired beams attacked by uniform corrosion and pitting were also carried out. The cross section area of the tensile reinforcement were reduced by 25% (uniform corrosion) over a length equal to 50% of the span of the beams. In addition, the cross section of the tensile reinforcement were also reduced by 38% due to pitting. The pits were located at the centre of the beams. The calculated ultimate load was equal to the SLS load of 31.8 kN/m which is only 77% of the ULS load of 41.3 kN/m.

7. REFERENCES

1. Horrigmoe, G. and Tørhlen, A. (1998) Load-carrying capacity of damaged and repaired concrete beams, *Concrete Under Severe Conditions 2 - Environment and Loading*, (eds. O. E. Gjorv, K. Sakai and N. Banthia), E&FN Spon, London, Vol. 2, pp. 1075-1085.
2. Horrigmoe, G. (1999) Computer modelling of damaged and repaired concrete structures, *Proceedings of the European Conference on Computational Mechanics (ECCM'99)*, Munich, Germany.
3. Rodriguez J., Ortega L. M., Casal J. and Diez: Corrosion of reinforcement and service life of concrete structures, *Proceedings of the Seventh International Conference on Durability of Building Materials and Components, Volume one: Prediction, Degradation and Materials*, Stockholm, Sweden, 1996.
4. Rodriguez J., Ortega L. M., Garcia, A. M.: Corrosion of reinforcing bars and service life of reinforced concrete: corrosion and bond deterioration, *International Conference Concrete across borders*, Odense, Denmark, 1994.
5. Comite Euro-International du Beton: CEB-FIP Model code 1990, Thomas Telford, London, 1993.
6. Castellani A. and Coronelli, D.: Beams with corroded reinforcement: Evaluation of the effects of cross-section losses and bond deterioration by finite element analysis, *Structural Faults and Repair, 8th International Conference on Extending the Life of Bridges, Civil and Building structures*, London, Juli, 1999.
7. Tørhlen, A.-and Horrigmoe, G.: Modeling bond between reinforcement and concrete in deteriorated and repaired beams (in Norwegian), Report NTAS A98034, NORUT Teknologi as, Narvik, Norway, 1998.
8. Norwegian code: Concrete structures, Design rules, NS 3473, (in Norwegian), 5. Edition, November, 1998.